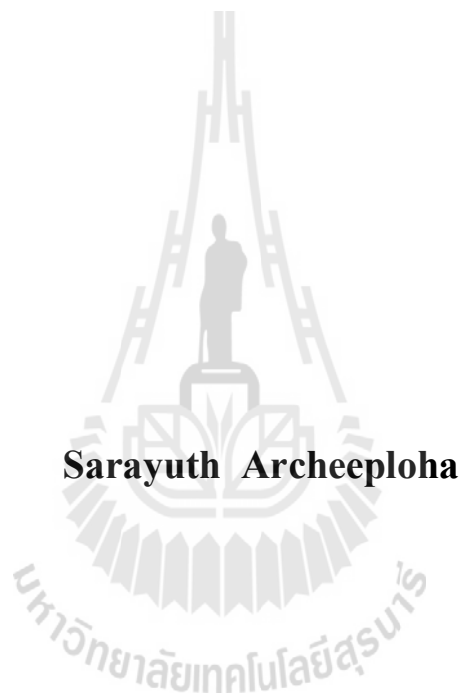# EFFECTS OF THERMAL AND MECHANICAL CYCLIC

LOADS ON TIME-DEPENDENT BEHAVIOR

OF ROCK SALT

Sarayuth Archeeploha

A Thesis Submitted in Partial Fulfillment of the Requirements for the

Degree of Doctor of Philosophy of Engineering in Geotechnology

Suranaree University of Technology

Academic Year 2014

ผลกระทบของการให้อุณหภูมิและแรงแบบวัฏจักร
ต่อพฤติกรรมเชิงเวลาของเกลือหิน

นายสรายุทธ อาชีพโลหะ

วิทยานิพนธ์นี้เป็นส่วนหนึ่งของการศึกษาตามหลักสูตรปริญญาวิศวกรรมศาสตรดุษฎีบัณฑิต
สาขาวิชาเทคโนโลยีธรณี
มหาวิทยาลัยเทคโนโลยีสุรนารี
ปีการศึกษา 2557

EFFECTS OF THERMAL AND MECHANICAL CYCLIC LOADS

ON TIME-DEPENDENT BEHAVIOR OF ROCK SALT

Suranaree University of Technology has approved this thesis submitted in partial fulfillment of the requirements for the Degree of Doctor of Philosophy.

Thesis Examining Committee

_____

(Dr. Decho Phueakphum)

Chairperson

_____

(Prof. Dr. Kittitep Fuenkajorn)

Member (Thesis Advisor)

_____

(Dr. Prachya Tepnarong)

Member

_____

(Dr. Anisong Chitnarin)

Member

_____

(Assoc. Prof. Ladda Wannakao)

Member

_____   _____

(Prof. Dr. Sukit Limpijumnong)   (Assoc. Prof. Flt. Lt. Dr. Kontorn Chamniprasart)

Vice Rector for Academic Affairs   Dean of Institute of Engineering

and Innovation

สรายุทธ อาชีพโลหะ : ผลกระทบของการให้อุณหภูมิและแรงแบบวัฏจักรต่อพฤติกรรม
เชิงเวลาของเกลือหิน (EFFECTS OF THERMAL AND MECHANICAL CYCLIC
LOADS ON TIME-DEPENDENT BEHAVIOR OF ROCK SALT)
อาจารย์ที่ปรึกษา : ศาสตราจารย์ ดร.กิตติเทพ เฟื่องขจร, 86 หน้า

วัตถุประสงค์ของการศึกษานี้คือเพื่อหาผลกระทบของอุณหภูมิต่อค่าความแข็ง และความ
ยืดหยุ่นของเกลือหินและผลกระทบของวัฏจักรการให้แรงและอุณหภูมิต่อพฤติกรรมการคืบของ
เกลือหิน โดยมีการทดสอบคุณสมบัติพื้นฐาน การคืบในแกนเดียว และการทดสอบการให้แรง
แบบวัฏจักร รูปแบบของ Burgers ได้นำมาใช้วิเคราะห์ผลการทดสอบเพื่อหาสัมประสิทธิ์การไหล
แบบพลาสติกภายใต้การให้แรงแบบสถิตย์และแบบวัฏจักร ผลการทดสอบระบุว่าวัฏจักรการให้
แรงและอุณหภูมิ (MTCL) จะให้ค่าความเครียดคืบสูงกว่าการให้แรงแบบสถิต การจำลองโดยใช้
โปรแกรม FLAC เพื่อศึกษาพฤติกรรมของโพรงกักเก็บอากาศอัดในเกลือหินระบุว่าการหดตัวของ
โพรงภายใต้สภาวะ MTCL มีค่าประมาณร้อยละ 22 สูงกว่าการหดตัวภายใต้สภาวะความเค้นสถิต
ผลการคำนวณโดยใช้สมการสำเร็จรูปให้ค่าการหดตัวเท่ากับร้อยละ 26 ซึ่งสูงกว่าผลที่จำลองได้จาก
โปรแกรม FLAC ผลการศึกษานี้ระบุว่าการทดสอบและการจำลองการหดตัวของโพรงกักเก็บ
ภายใต้สภาวะ MTCL สามารถให้ผลในเชิงอนุรักษ์เมื่อเทียบกับการทดสอบและการวิเคราะห์แบบ
ดั้งเดิมที่ทำมาในอดีต

สาขาวิชา เทคโนโลยีธรณี   ลายมือชื่อนักศึกษา _____
ปีการศึกษา 2557   ลายมือชื่ออาจารย์ที่ปรึกษา _____

SARAYUTH ARCHEEPLOHA : EFFECTS OF THERMAL AND
MECHANICAL CYCLIC LOADS ON TIME-DEPENDENT BEHAVIOR
OF ROCK SALT. THESIS ADVISOR : PROF. KITTITEP
FUENKAJORN, Ph.D., P.E., 86 PP.

ROCK SALT / TEMPERATURE / STEADY-STATE / VISCO-PLASTICITY /
STORAGE CAVERN

The objectives of this study are to determine temperature effect on salt strength and elasticity and the effects of mechanical and thermal loading cycles on the steady-state creep behavior of the Maha Sarakham salt. Basic mechanical tests and uniaxial creep and cyclic loading tests have been performed. The calibration of the steady-state creep phase using the Burgers model can determine the visco-plastic coefficient under static and cyclic loading (MSL and MCL tests). The mechanical and thermal cyclic loading (MTCL) induces a higher creep strain than does the static loading. The simulations of the compress-air storage caverns by FLAC indicate that the cavern closure under MTCL condition is about 22% greater than that under static loading condition. The calculation result from closure equation provide the cavern closure of 26% which slightly higher than those the result from FLAC. This suggests that salt testing and simulation of the storage caverns under MTCL condition can provide a more conservative assessment of the cavern closure than those obtained from the conventional creep testing.

School of Geotechnology   Student's Signature_____

Academic Year 2014   Advisor's Signature_____

ACKNOWLEDGMENTS

I would like to express my sincere thanks to Prof. Dr. Kittitep Fuenkajorn, thesis advisor, who gave a critical review and constant encouragement throughout the course of this research. Further appreciation is extended to Dr. Decho Phueakphum : Chairman, School of Geotechnology, Prof. Dr. Kittitep Fuenkajorn, thesis advisor, School of Geotechnology, Prof. Dr. Suksun Horpibulsuk, School of Civil engineering, Dr. Prachya Tepnarong, School of Geotechnology, Suranaree University of Technology (SUT) and Assoc. Prof. Ladda Wannakao, Department of Geotechnology, Faculty of Technology, Khon Kaen Unviersity (KKU) who are member of my examination committee. Grateful thanks are given to all staffs of Geomechanics Research Unit, Institute of Engineering who supported my work.

Finally, I most gratefully acknowledge my parents and friends for all their supported throughout the period of this study.

Sarayuth Archeeploha

LIST OF TABLES

LIST OF FIGURES

LIST OF FIGURES (Continued)

LIST OF FIGURES (Continued)

LIST OF TABLES

LIST OF FIGURES

LIST OF FIGURES (Continued)

LIST OF FIGURES (Continued)

SYMBOLS AND ABBREVIATIONS

a	=	hole radius or inner boundary
A and B	=	time-independent functions of position
E or E_1	=	Elastic modulus
E_2	=	Visco-elastic modulus
K	=	bulk modulus
K	=	stress ratio (σ_y/σ_x)
P_i	=	Internal pressure
P_o	=	External pressure
r	=	radius
T	=	Temperature (Kelvin)
t	=	time (Day)
V	=	Poisson's ratio
α	=	time-dependent function
ε_1	=	Axial strain
$\varepsilon_2, \varepsilon_3$	=	Lateral strain
ν	=	Poisson's ratio
σ_1	=	Maximum principal stress
σ_2	=	Intermediate principal stress

SYMBOLS AND ABBREVIATIONS (Continued)

σ_3	=	Minimum principal stress
σ_o	=	Yield stress
τ_{oct}	=	Octahedral shear stress
η_1	=	Visco-plastic viscosity
η_2	=	Visco-elastic viscosity
θ	=	tangential coordinate
σ_B	=	Brazilian tensile strength
σ_c	=	Uniaxial compressive strength
σ_x, σ_y	=	lateral stresses
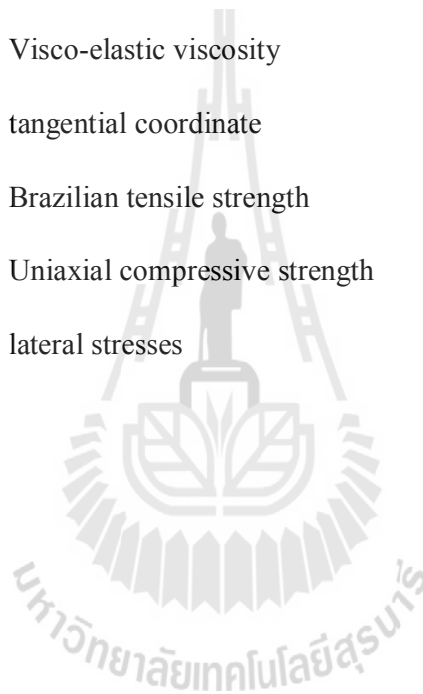
CHAPTER I

INTRODUCTION

1.1   Background and rationale

One of the problems involving in the compressed-air, liquefied petroleum and natural gas storage in salt caverns is the effect of temperature and stress changes in the surround salt due to the injection-withdrawal cycles. The differential stresses around the cavern during product injection periods decrease while the temperature increases. During product retrieval periods the stresses increase while the temperature decreases. The conventional creep tests at which the salt specimens are subjected to constant ambient or elevated temperatures may not truly represent the actual salt behavior under the storage conditions. Even though the effects of mechanical cyclic loading on the time-dependent behavior of salt have been recognized and studied, the effects of the alternated mechanical and thermal loadings on the creep behavior of the salt have never been assessed.

1.2   Research objectives

The objective of this study is to determine the effects of the alternated cycles of thermal and mechanical loadings on the time-dependent deformation and strength of rock salt obtained from the Maha Sarakham formation. A uniaxial load frame is used to apply constant axial stresses to the cylindrical salt specimens with a nominal diameter of 100 mm. The testing temperatures range from 25 to 100 °C. FLAC is used to simulate the cavern deformability and strength under thermal and mechanical cyclic

loads. The results will be used to determine of the cavern stability unde storage condition.

1.3 Research methodology

The research methodology shown in Figure 1.1 comprises 7 steps; including literature review, sample preparation, laboratory testing, computer simulation, discussions and conclusions and thesis writing.

1.3.1 Literature review

Literature review is carried out to study the previous researches on time-dependent behavior of rock salt, and mechanical and thermal properties. The sources of information are from text books, journals, technical reports and conference papers. A summary of the literature review will be given in the thesis.

1.3.2 Sample preparation

Rock salt samples have been donated by Asean Potash Mining Co. from the Khorat basin, northeast of Thailand. The salt cores belong to the Middle member of the Maha Sarakham formation (Warren, 1999). The salt cores used here are virtually pure halite with average grain (crystal) sizes of $5\times5\times10$ mm^3. Samples are prepared for basic strength tests, cyclic loading tests, and uniaxial creep test. The salt specimens are cylindrical shaped with 100 millimeters in diameter for cyclic loading tests, and uniaxial creep test under thermal loading. For the mechanical testing the cores are dry-cut to obtain cubical shaped specimens with nominal dimensions of $5.4\times5.4\times5.4$ cm^3. The Brazilian test specimens are machined using a lathe to obtain

Literature Review

↓

Sample Preparation

↓

Laboratory Tests

Uniaxial Creep Tests

Uniaxial Cyclic Loading Tests

Basic Property Tests

Elevated Temperatures

Ambient Temperature

High Thermal Cyclic loading

Ambient Temperature Cyclic loading

Thermal and Mechanical Cyclic loading

Derivation of the Relationships between Thermal and Mechanical Loadings with Salt Behavior

↓

Computer Simulations

↓

Discussions and Conclusions

↓

Thesis Writing

Figure 1.1 Research methodology

48 mm diameter circular disks with a thickness of 24 mm. Preparations of these samples will follow as much as practical the American Society for Testing and Materials (ASTM D4543).

1.3.3 Laboratory testing

Laboratory tests include uniaxial and triaxial compressive strength tests, triaxial compression test, Brazilian tensile strength test, cyclic loading test, and uniaxial creep test under thermal loading. The test series include the basic strength tests as follows; 1) five specimens of uniaxial compressive strength test (ASTM D2938), 2) five specimens of Brazilian tensile strength test (ASTM D3967), 3) and nine specimens of triaxial compressive strength test (ASTM D2664). Three specimens will be used for uniaxial cyclic loading test and three specimens for the uniaxial creep test (ASTM D4405 and ASTM D7070-08).

The uniaxial creep is performed under thermal and mechanical loading. A consolidation loading frame is used to apply constant axial stresses to the cylindrical salt specimens. It is divided as follows:

1) The mechanical and thermal cyclic loading (MTCL) tests by applied the elevated and low temperatures with normal loads varied from 20 to 50% of the salt strength on the specimens. Salt specimens are heated under low normal load at 1 MPa for one cycle. The temperature is reduced under high normal load at selected axial stresses (20 to 50% of salt strength) for another cycle. Figure 1.2 is shows the alternated mechanical and thermal loadings respect to time.

2) The mechanical static loading (MSL) is tested under elevated temperature creep tests with constant axial load from 20 to 50% of the salt strength.
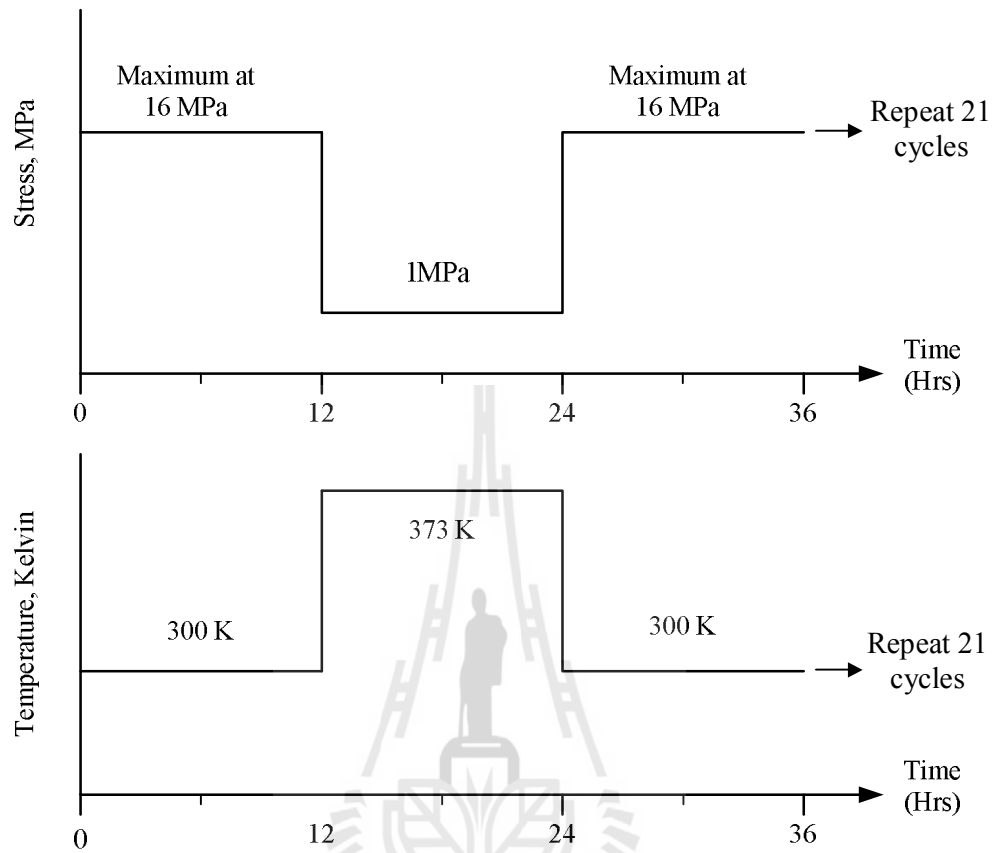
Figure 1.2 Elevated and low temperatures with normal loads varied from 1 MPa to selected axial stresses from 20 to 50% of the salt strength during the tests.

      3) The mechanical static loading is tested ambient temperature creep test with constant axial load from 20 to 50% of the salt strength.

      4) The mechanical cyclic loading (MCL) is tested under ambient temperature

      5) The MCL is tested under elevated temperatures at 100 °C.

The cyclic loadings are tested with axial stresses varied from 1 to selected axial stresses from 20 to 50% of the salt strength. The vertical and lateral deformations are monitored using dial gages during the tests. A heating tape with temperature regulator is used to constant the temperature of the specimens. All tests are performed for 21 days.

1.3.4 Mathematical relations

The results are used to describe the deformability and strength of salt rock specimens, elastic modulus, Poisson's ratio, and stress-strain with time dependency under thermal and mechanical cyclic loads. The results are used to calibrate the elastic, visco-elastic and visco-plastic parameters of the rock under mechanical static loading, mechanical cyclic loading and mechanical and thermal cyclic loading.

1.3.5 Computer simulations

The creep parameters calibrated from various cases are used to assess the stability of natural gas storage cavern by using closed-form solution and finite difference code (FLAC 4.0). A finite element analysis will be performed for various cavern geometries to demonstrate the impact of thermal and cyclic loading on the salt behavior around a natural gas storage caverns subjected to cycles of pressure injection and retrieval.

1.3.6 Discussions, conclusion and thesis writing

Discussions are made to analyze the impacts of the thermal and mechanical cyclic loads on the storage cavern stability. All research activities, methods, and results will be documented and complied in the thesis. The research or findings will be published in the conference proceedings or journals.

1.4 Scope and limitations

The scope and limitations of the research include as follows.

1. All testing are conducted on rock salt specimens obtained from the Maha Sarakham formation. The rock salt is relatively pure halite with slight amount (less than 1-2%) of anhydrite, clay minerals and ferrous oxide.

2. Basic characterization tests are performed, including uniaxial and triaxial compressive strength tests and Brazilian tensile strength tests. The testing temperatures range from 25 to 100 °C. The test procedures will follow the relevant ASTM standard practices.

3. Series of uniaxial creep tests are performed with the applied axial stresses varying from 20 to 50% of the salt strength. Testing temperatures for the creep testing range from 25 to 100 °C. Up to 3 samples will be tested for each temperature. The test procedure follows the ASTM standard practice.

4. All creep tests will be performed up to 21 days or 21 cycles.

5. All testing will be made under dry condition.

6. No field testing will be performed.

7. Numerical simulations using FLAC will be performed to study the salt creep around natural gas storage caverns.

1.5 Thesis contents

This research thesis is divided into six chapters. The first chapter includes background and rationale, research objectives, research methodology, and scope and limitations. Chapter II presents results of the literature review to the previous research on factors affecting rock salt behavior. Chapter III describes sample preparation.

Chapter IV conventional and cyclic creep tests are performed to obtain the creep parameters. Chapter V shows the test results. Chapter VI presents creep calibrations and numerical simulations. Chapter VII is the discussions, conclusions and recommendations for future studies.
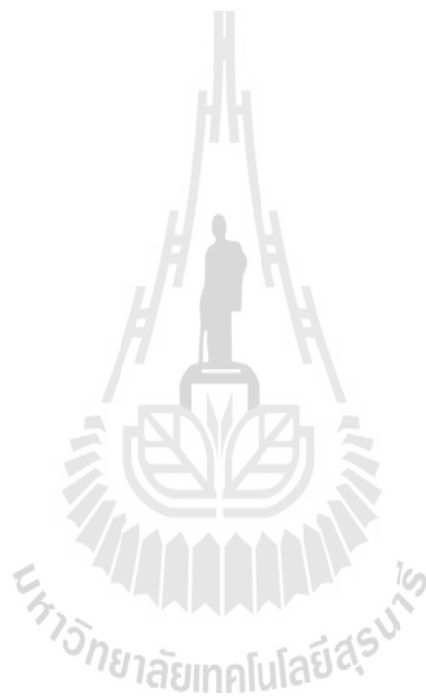
CHAPTER II

LITERATURE REVIEW

2.1   Introduction

This chapter summarizes the results of literature review carried out to improve an understanding of effects of time-dependent behavior of rock salt, mechanical and thermal properties. The topics reviewed here are factors affecting rock salt behavior and thermomechanical effects.

2.2   Factors affecting rock salt behavior

The mechanical behavior of rock salt is complex and is affected by many factors, such as grain size, bonding between grains, time, temperature, humidity, and inclusions, and more. The effects on rock salt characteristics by these factors are normally shown by the differences in deformation and creep properties.

The effects of grain size on the creep behavior and strength of rock salt in laboratory and field conditions are described by Fokker (1998). The average grain size of salt visually observed from the core and post-failure specimens is 5×10×10 millimeters. It is concluded that the large size of the salt crystals increases the effect of the crystallographic features (i.e. cleavage planes) on the mechanics of deformation and failure of the samples. This also agrees with the finding by Aubertin (1996). The dislocations and plastic flows in single crystals of halite are studied by several researchers (Franssen and Spiers, 1990; Raj and Pharr, 1992; Senseny et al., 1992;

Wanten et al., 1996). They conclude that the shear strength and deformation of halite crystals are orientation-dependent. The small size of the sample may not provide good representative test results. This also reflects on the specifications by ASTM (ASTM D2664, D2938, and D3967). The ASTM standard methods specify that to minimize the effect of grain size the sample diameter should be at least ten times the average grain size.

Bonding between grains can affect the creep rate and the strength of salt. Allemandou and Dusseault (1996) observed the post-failure from the Brazilian strength tests and uniaxial compressive strength tests. They report that strength depends on the boundary between grains. This also agrees with the laboratory results obtained by Fuenkajorn and Daemen (1988) who reported that weakness or brittleness of the crystal boundary of salt is observed during sample preparation. It is unlikely that a long intact core can drill through the salt formation.

The time-dependent behavior of salt under differential stress raises the question of the significance of time-related test parameters such as loading rate, testing period, and loading sequence. The effects of stress rate and strain rate on the deformation and strength of salt samples have long been recognized (Farmer and Gilbert, 1984; Dusseault and Fordham, 1993). The loading rate must be maintained constant and measured as precisely as possible during the test. The loading sequence and the duration for which each load is sustained by the salt specimens are important since salt tends to behave as a plastic creep material with low yield stress. This situation is found in the triaxial compressive strength test where the confining pressure is applied to the salt cylinder prior to the axial load. Due to the nonlinear behavior of

salt, the analysis of stress induced in a salt specimen is complex and the Boltzmann law of superposition cannot be used.

Samsri et al. (2010) determined the effect of the intermediate principal stress on the time-dependent behavior of rock salt obtained from the Maha Sarakham formation. A polyaxial creep frame applies constant principal stresses to cubical shaped specimens with a nominal dimension of $5.4 \times 5.4 \times 5.4$ cm^3. The applied octahedral shear stresses (τ_{oct}) vary from 5, 8, 11 to 14 MPa while the mean stress (σ_m) is maintained constant at 15 MPa for all specimens. The loading conditions range from the triaxial ($\sigma_1 \neq \sigma_2 = \sigma_3$) to the polyaxial ($\sigma_1 \neq \sigma_2 \neq \sigma_3$ and $\sigma_1 = \sigma_2 \neq \sigma_3$) stress states. The Burgers model is used to describe the elastic, visco-elastic (transient) and visco-plastic (steady-state) behavior of the salt. The specimen deformations are monitored along the three principal axes for up to 21 days. Regression analyses on the octahedral shear strain - time curves suggest that the salt elastic modulus tends to be independent of the intermediate principal stress (σ_2). It however tends to increase as the applied τ_{oct} increases. Under the same magnitude of τ_{oct} the visco-elastic and visco-plastic parameters increases when σ_2 increases from the triaxial condition, $\sigma_2 = \sigma_3$, to the condition where $\sigma_2 = \sigma_1$.

Samsri et al. (2011) studied the polyaxial (true triaxial) creep testing has been performed to determine the effect of the intermediate principal stress on the time-dependent behavior of rock salt obtained from the Maha Sarakham formation. A polyaxial creep frame applies constant principal stresses to cubical shaped specimens with a nominal dimension of $5.4 \times 5.4 \times 5.4$ cm^3. The applied octahedral shear stresses (τ_{oct}) vary from 5, 8, 11 to 14 MPa while the mean stress (σ_m) is maintained constant at 15 MPa for all specimens. The loading conditions range from the triaxial

$(\sigma_1 \neq \sigma_2 = \sigma_3)$ to the polyaxial $(\sigma_1 \neq \sigma_2 \neq \sigma_3$ and $\sigma_1 = \sigma_2 \neq \sigma_3)$ stress states. The Burgers model is used to describe the elastic, visco-elastic (transient) and visco-plastic (steady-state) behavior of the salt. The specimen deformations are monitored along the three principal axes for up to 21 days. Regression analyses on the octahedral shear strain - time curves suggest that the salt elastic modulus tends to be independent of the intermediate principal stress (σ_2).

The effect of cyclic loading on the elasticity and strengths of geologic materials has long been recognized (Haimson, 1974; Bagde & Petros, 2005). Liang et al. 2012 studied the mechanical properties of rock samples under monotonic and cyclic loadings. Under cyclic loading, the strain of rock salt at the peak strength increases by 1.98%, twice more than that under monotonic loading. Most studies aims to determine the fatigue strength of the materials. It has been found that loading cycles can reduce the material strength and elasticity, depending on the loading amplitude and the maximum applied load in each cycle (Zhenyu & Haihong, 1990; Singh et al., 1994; Ray et al., 1999; Kodama et al., 2000; Bauer et al., 2011). Storage caverns are usually located deep underground and the temperature and confining pressure may increase considerably with depth. The injection-withdrawal rate is caused the temperature changes in salt storage (Berest et al., 2013; Kushnir et al., 2012). The effects of temperature on deformability and strength of rocks have long been recognized (Vosteen & Schellschmidt, 2003; Shimada & Liu, 2000; Okatov et al., 2003)

Fuenkajorn and Phueakphum (2010) performed cyclic loading tests on the Maha Sarakham salt. Their results indicate that the salt compressive strength decreases with increasing number of loading cycles, which can be best represented by

a power equation. The salt elastic modulus decreases slightly during the first few cycles, and tends to remain constant until failure. It seems to be independent of the maximum loads. Axial strain–time curves compiled from loci of the maximum load of each cycle apparently show a time-dependent behavior similar to that of creep tests under static loading. In the steady-state creep phase, the visco-plastic coefficients calculated from the cyclic loading test are about an order of magnitude lower than those under static loading. The salt visco-plasticity also decreases with increasing loading frequency. Surface subsidence and cavern closure simulated using parameters calibrated from cyclic loading test results are about 40% greater than those from the static loading results. This suggests that application of the property parameters obtained from the conventional static loading creep test to assess the long-term stability of storage caverns in salt with internal pressure fluctuation may not be conservative.

Sriapai et al. (2011) studied the uniaxial and triaxial compression tests have been performed on Maha Sarakham salt to assess the influence of loading rate on the compressive strength of the rock. The salt specimens with a nominal dimension of $5.4 \times 5.4 \times 5.4$ cm^3 are compressed to failure using a polyaxial load frame. The lateral confining pressures are maintained constant at 0, 3, 7, 12, 20 and 28 MPa while the axial stresses are applied at constant rates of 0.001, 0.01, 0.1, 1.0 and 10 MPa/s. The salt strengths exponentially increase with the loading rates. The effect is more pronounced under high confining pressures.

Temperature or heating affects the creep deformation, because they increase the plastic property of salt and long-term deformation (Pudewills et al., 1995). Jeremic (1994) postulated that rock salts lose their brittleness after extension

tempering at approximately 600 °C and exhibit a critical shear stress up to 1 MPa. Hamami et al. (1996) study the effect of temperature and conclude that the temperature increase, as for the deviatoric stress, results in an increase of the material deformation. Cristescu and Hunsche (1996) study the temperature effect on the strain rate suitable for laboratory testing. They suggest that the appropriate strain rate for testing at 100 °C and 200 °C is 10^{-8} s^{-1} and 10^{-7} s^{-1} because the temperature can affect the creep deformation and strength of salt under high temperatures.

Inada et al. (1997) studied the temporary storage of high and low temperature materials in openings excavated in rock mountain from the view point of efficient utilization of land and preservation of the environment. In this case, high temperature materials means such as heated water which is produced by surplus heat from garbage burning plants, and low temperature materials means such as LNG, LPG, frozen food etc. Heated water, LNG and LPG actually are stored in openings, as the quantity of these materials changes continually, the rock mass around openings will receive the effects of thermal hysteresis of high and low temperatures. Therefore, obtaining the strength and deformation characteristics of rock after undergoing thermal hysteresis of high and low temperatures becomes important for discussing the stability of the openings. In this study, strength and deformation characteristics of rock which has low and high porosity were examined after undergoing thermal hysteresis of high and low temperatures using a thermal cycle apparatus. From the results, it was found that temperature, the number of hysteresis and porosity etc. were important factors which have an influence on strength and deformation characteristics. The main results obtained in this study are as follows;

Compressive and tensile strength of rocks decrease with the increasing number of thermal hysteresis. However, the ratio of decreasing decreases. From, this fact, it is supposed that the value will converge to a constant value. The values of tangential Young's modulus and Poisson's ratio of rocks after undergoing thermal hysteresis have the same tendency as those of compressive and tensile strength. From the results of measuring strain, the residual strains at room temperature can be seen for all specimens after undergoing thermal hysteresis. However, it is considered that the residual strain tends to converge to a constant value as thermal hysteresis is repeated. Elastic wave propagation velocity of rocks decreases with the increasing number of thermal hysteresis, but the ratio of decreasing decreases. It is considered that the value will converge to a constant value.

Yang and Daemen (1997) investigation and explanation are given of temperature effects on creep of tuff. Creep tests have been conducted at room temperature and at elevated temperature (204 °C). In order to model the creep behavior of tuff, a new time-dependent damage model and two definitions of stress intensity factor are proposed. The results of experiments and theoretical analysis show that the creep strain of tuff increases with increasing temperature under the same loading condition, and that the stress intensity factor is not only a function of stress states, but also of temperature.

Yavuz et al. (2010) studied the thermal effect on the physical properties of carbonate rocks. The effect of thermal damage on the physical properties of five carbonate rocks has been investigated. The tests were con ducted on two marbles and three limes tones, mainly composed of calcite but with different grain sizes, porosities, structural and textural characteristics. Cubic samples prepared from these rocks were

gradually heated to a specific temperature level of 100, 200, 300, 400 and 500 °C, and gradually cooled down to room temperature without causing thermals hock in order to investigate the effect of heating temperature on physical properties such as microstructure, bulk density, effective porosity and P-wave velocity. Microscopic investigations from thin sect ions showed that damage in rock s at elevated temperatures was induced in different severity depending on grain size, porosity, structural and textural characteristics. Color changes were also ob served in porous limes tones (Lymra and Travertine) due to organic material. In accordance with the degree of calcite dilation depending on heating temperature and in turn new microcrack occurrence, separation along intragrain and/or intergrain boundaries and widening of existing cracks, P-wave velocity decreased to various levels of the initial value, whereas porosity increased. Microscopic analyses and P-wave velocity measurements indicate that compaction of rock structure up to 150 °C occurred and induced calcite dilation had no significant damage effect on the rock material. Compact ion of rock structure led to an increase in P-wave velocity and slight decrease in porosity. Most of the damage occurred within 24 h of heating time and further heating treatments brought relatively minor changes in physical properties. Damage intensity was well explained with P-wave velocity and effective porosity values depending on temperature increase.

Furong et al. (2011) studied the limestone specimens at 700 °C in uniaxial compression were carried out to investigate the mechanical effects of loading rates on limestone by using a MTS810 rock mechanics servo-controlled testing system considering the loading rate as a variable. The mechanical properties of limestone such as the stress–strain curve, variable characteristics of peak strength and the

modulus of elasticity of limestone were studied under the strain rates ranging from 1.1×10^{-5} to 1.1×10^{-1} s^{-1}. Sharp decreases were shown for the peak strength and elastic modulus of limestone from 1.1×10^{-5} to 1.1×10^{-4} s^{-1} at 700 °C as well as a downward trend was shown from 1.1×10^{-4} to 1.1×10^{-1} s^{-1} with the rise of the strain rate. The peak strain increased from 1.1×10^{-5} to 1.1×10^{-4} s^{-1}, however, there was no obvious changes shown for the peak strain of limestone from 1.1×10^{-4} to 1.1×10^{-1} s^{-1}. These results can provide valuable references for the rock blasting effect and design of mine.

Humidity affects salt properties by reducing the strength of rock salt (Hunsche and Schulze, 1996; Cleach et al., 1996). Hydrated reaction between water and salt occurs when salt contacts with air humidity. The temperature effects can catalyze the hydration. They find that when subjecting to air humidity, the strength of salt can be decreased by up to 1 MPa (normally, strength of 30 MPa).

Inclusions and impurities in salt have an effect on to the creep deformation and strength of salt. The degree of impurity is varying for different scales of the rock salt. On a small scale, such as for laboratory specimens, the impurities of salt involve ferruginous inclusions and thin clay seams along grain boundaries or bedding planes. The impurities distribute uniformly in the salt may affect the strength of rock salt. This can decrease the creep deformation and strength of rock salt. These phenomena have been reported by Franssen and Spiers (1990), Raj and Pharr (1992) and Senseny et al. (1992).

Kensakoo (2006) studied the relationship between the uniaxial compressive and Brazilian tensile strengths, elastic modulus and visco-plasticity coefficient of rock salt specimens and their mineralogical compositions and petrographic features. The main inclusions for the salt specimens tested here are anhydrite and clay minerals.

The anhydrite inclusions appear as thin seams or beds perpendicular to the core axis with thickness varying from few millimeters to several centimeters. The clay minerals (about 1-5% by weight) scatter between the salt crystals of some specimens. The compressive strength of the salt specimens linearly increases from 27 MPa to about 40 MPa as the anhydrite inclusion increases in the range from 0% to nearly 100%. This is primarily because the anhydrite inclusion makes the salt portion shorter, creates the end effect, and hence increasing the specimen strength. The combined effect between the salt and anhydrite properties also causes the increase of the specimen elasticity from 22 GPa to as high as 36 GPa. Tensile strengths of the salt specimens will also increase with the anhydrite inclusion if the inclusion is beyond 50% by weight. The clay content of less than 4% has no significant impact on the salt tensile strength. The effect of clay content beyond 5% in the salt specimens remains unclear because the range of the clay contents among different specimens are relatively low and narrow (0- 5%).

Fuenkajorn et al. (2011) studied the intrinsic variability of rock salt specimens obtained from the Middle and Lower members of the Maha Sarakham formation in the Khorat basin. Prior to the mechanical tests, the types and amount of inclusions were identified by visual examination and after testing by X-ray diffraction and dissolution methods. The uniaxial compressive strength of the specimens linearly increases from 27 MPa to about 40 MPa as the anhydrite content (by weight) increases from 0% (pure halite) to 100% (pure anhydrite). The combined stiffness of the salt and the anhydrite causes an increase of specimen elasticity from 22 GPa (pure salt) to as high as 36 GPa (pure anhydrite). Tensile strengths increase with increasing anhydrite content, particularly when the content is above 60% by weight. Below this

limit the anhydrite has an insignificant impact on the specimen tensile strength. The tensile strength of salt crystals can be as high as 2 MPa, whereas that of the inter-crystalline boundaries is 1 MPa. The visco-plasticity increases exponentially with crystal size, as dislocation glide mechanisms become predominant for the specimens comprising large crystals. Salt specimens with fine crystals deform by dislocation climb mechanisms, and hence reduce the specimen's visco-plasticity.

2.3   Thermomechanical effects

Pudewills and Droste (2003) studied the numerical simulation of the thermal and thermomechanical response of the large-scale in situ experiment ''thermal simulation of drift emplacement'', which was carried out in the Asse salt mine in Germany, is presented. The analyses concern the modeling of the temperature fields, thermally induced drift closure followed by the consolidation of backfill material and the distribution of the stresses. Finite element codes (ADINA and MAUS) specially developed for the repository structures as well as a general-purpose code have been used. The primary objective of the investigations is to evaluate the capability of these codes to simulate the thermomechanical behavior of rock salt and backfill material under representative conditions of a waste repository by comparing of calculated results with in situ measurements. An overall good agreement between modeling and in situ measured results indicates that most thermomechanical effects are fairy well represented by the numerical models.

The thermomechanical behavior of rock salt was described in the finite element analyses by a thermoelastic material model with a temperature-dependent steady- state creep and based on the experimental results. According to this model,

the total strain rate is given as the sum of elastic, thermal, and steady-state creep rates. This constitutive relation governing the creep strain rate of rock salt is described as follows:

$$\varepsilon_{ef} = A\sigma^5_{ef} \exp(-Q/(RT)) \tag{2.1}$$

Dwivedi et al. (2008) studied the thermo-mechanical and transport properties of granites which is required to understand and model a number of processes in the earth crust such as folding, geothermal activity, magmatic intrusions, plate tectonics and nuclear waste disposal. Thermo-mechanical properties of Indian granite (IG) is studied various at high temperatures in the range of 30–160 °C, keeping in view the highest temperatures expected in underground nuclear waste repositories. These properties are Young's modulus, uniaxial compressive strength, tensile strength, Poisson's ratio, coefficient of linear thermal expansion, creep behaviour and the development of micro-crack on heating using scanning electron microscope (SEM). The results is indicate that the temperature effect on creep under atmospheric pressure condition (0.1 MPa) was not observed up to 160 °C in the duration of 4 months for Indian pink granite. Permeability decreases with increase in temperature. Thermal conductivity and thermal diffusivity both decrease with increase in temperature. The de crease in thermal conductivity with temperature is high on increase of the confining pressure. On the other hand, specific heat increases with increase in temperature and pressure up to 600 °C and the coefficient of linear thermal expansion increases with temperature up to 470 °C. Viscosity of molten granite decreases with increase in temperature. Ultimate compressive strength increases with increase in confining pressure. On the other hand, tensile strength of all granites decreases with increase in

temperature for the reported temperature range 30–1050 °C. Normalized cohesion (c/c_0) and normalized angle of internal friction (ϕ/ϕ_0) both decrease with increase in temperature for all granites.

CHAPTER IV

LABORATORY TESTS

4.1 Introduction

The objective of this chapter is to experimentally determine the basic strengths of rock salt subjected to storage cavern condition. This chapter describes the equipment and method of the uniaxial compressive strength test, Brazilian tensile strength test, uniaxial creep test include the mechanical static loading (MSL), mechanical cyclic loading test (MCL) and, mechanical and thermal cyclic loading test (MTCL).

4.2 Mechanical testing

Due to the fact that the salt specimens must be tested under elevated temperatures, a polyaxial load frame (Sriapai et al., 2011; Fuenkajorn et al., 2012) has been used to apply axial stress and lateral stresses to the cubical salt specimens (Figure 4.1). The test frame utilizes two pairs of cantilever beams to apply lateral stresses to the specimen. The axial stress is applied by a hydraulic cylinder connected to an electric pump. The frame has an advantage over the conventional triaxial (Hoek) cell because it allows a relatively quick installation of the test specimen under triaxial condition, and hence the change of the specimen temperature during testing is minimal. A total of ten specimens have been tested for each temperature level with the confining (lateral) stresses varying from 0, 3, 5, 10, 15, 20 to 30 MPa. They are loaded axially at a constant rate of 1 MPa/s until failure occurs.
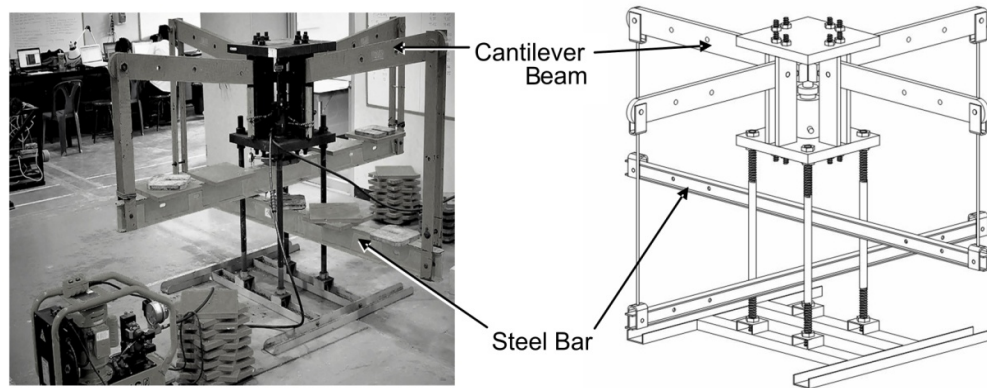
Figure 4.1 A polyaxial load frame (Sriapai et al., 2011; Fuenkajorn et al., 2012) used in the compressive strength testing of salt specimens under various temperatures.
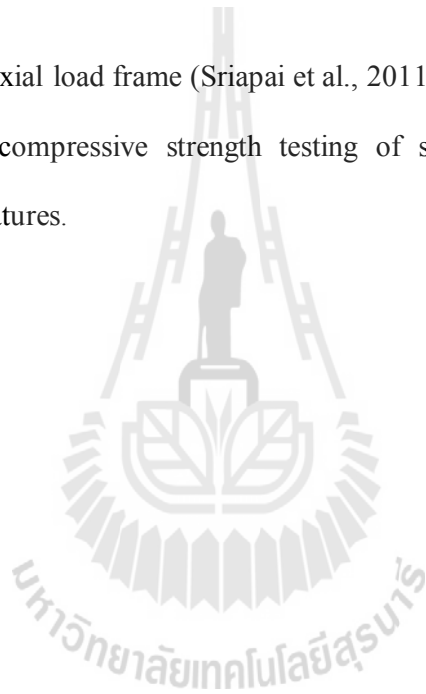
The Brazilian tensile strength of the salt has been determined from disk specimens with temperatures ranging from 273, 298, 404 to 467 Kelvin. Except the pre-heating and pre-cooling processes, the test procedure, sample preparation and strength calculation follow the ASTM (D3967-08) standard practice.

4.3 Creep testing

The test procedure and apparatus follow the ASTM D7070-08 standard practice as much as practical. A dead weight loading device applies a constant and uniform stress along the axial direction of the salt core specimen (Figure 4.2). Prior to testing the axial load is calibrated to obtain a desired axial stresses by using an electronic load cell. The axial loads are determined to obtain the maximum axial stresses ranging from 6.5, 10, 13 to 16 MPa (20% to 50% of the salt uniaxial compressive strength) or equivalent to the octahedral shear stresses (τ_{oct}) of 3.1, 4.53, 6.13 and 7.54 MPa. The test methods can be separated into 3 series as:

1. Mechanical static loading (MSL)

2. Mechanical cyclic loading (MCL)

3. Mechanical and thermal cyclic loading (MTCL)

For MSL testing, after installing the salt specimen into the consolidation load frame, dead weights are placed on the circular plate at the bottom connected to a steel rod on the other end of the fixed beam. Neoprene sheets are placed at the interface between loading platens and rock surfaces to minimize friction. For the elevated temperature, a heating tape with temperature regulator is used to maintain a constant specimen temperature. The specimen deformations are monitored by four dial gages with high precision (±0.01 mm) placed vertically and horizontally on the opposite
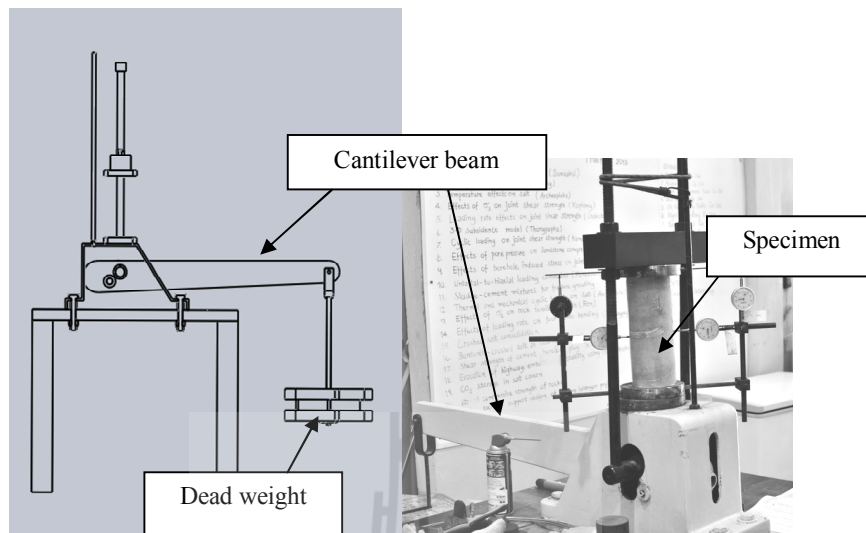
Figure 4.2 A salt specimen placed in the consolidation load frame.

sides of the specimen. The readings are recorded every 30 seconds, immediately after applying the axial load. The reading intervals are gradually increased to once every half hour after 3 hours of testing.

The MCL tests have been performed on the same specimens after the results under static load are recorded for 21 days. After 21 days under MSL testing the salt specimens are unloaded to the minimum stress of 1 MPa for 12 hours and reloaded to the selected axial stress for each specimen for 12 hours (Figure 4.3). This loading cycle is repeated 21 times (21 days).

The MTCL tests are performed by combining the effects of cyclic thermal and mechanical loadings. After the static loading under ambient temperature for 21 days, the salt specimens are unloaded to the minimum stress of 1 MPa under 373 K for 12 hours and reloaded to the selected axial stress under 300 K for 12 hours (Figure 4.4). The cyclic loading period is 21 days.
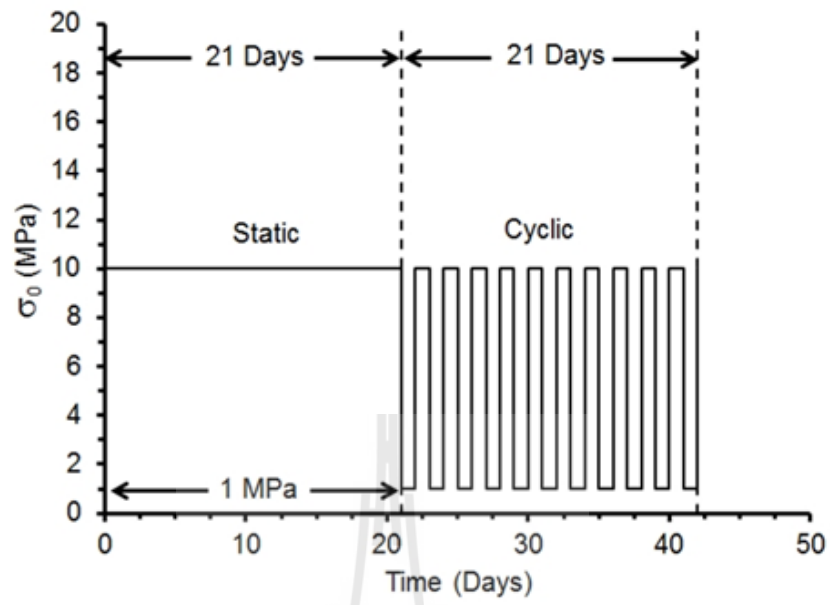
Figure 4.3 Static and cyclic loading paths as a function of time.
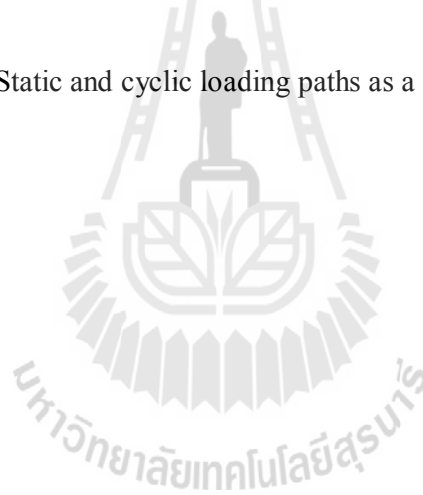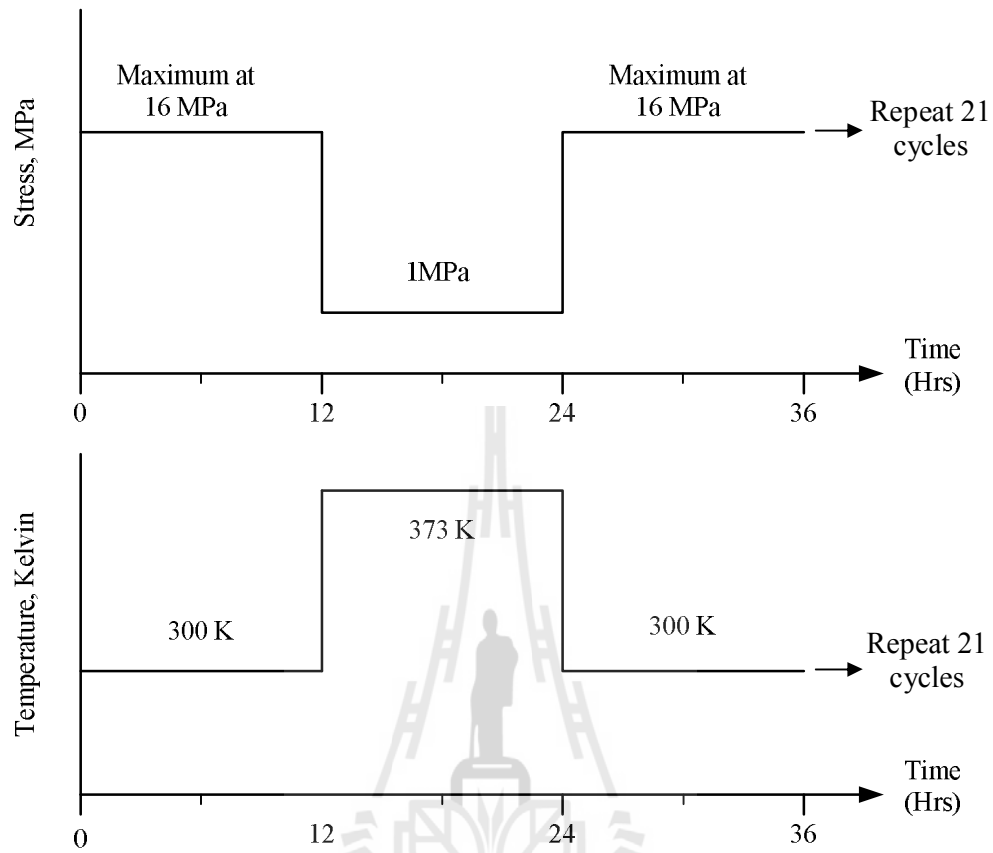
Figure 4.4 Stress and temperature path for MTCL testing (See text for explanation).

CHAPTER V

TEST RESULTS

5.1   Introduction

This chapter describes the laboratory test results of the uniaxial compressive strength, Brazilian tensile strength and, uniaxial creep tests. The load configurations of creep tests include mechanical static loading (MSL), mechanical cyclic loading (MCL) and, mechanical and thermal cyclic loading tests (MTCL).

5.2   Uniaxial compressive strength

For this test series the compressive strengths are determined for various temperatures from 277, 298, 394, to 456 Kelvin. The results are presented in the forms of uniaxial compressive strength as a function of temperature in Figure 5.1. The results indicate that the uniaxial compressive strengths (σ_c) of salt decrease linearly with increasing temperature (T) and can be represented best by:

$$\sigma_c = -67.1 \times 10^{-3}T + 56.7 \text{ MPa} \qquad ;T(\text{Kelvin}) \qquad (5.1)$$

Table 5.1 summarizes the compressive strengths of rock salt under various temperatures. This is indicated that the temperature can reduce the salt strength particularly, under high temperature level.
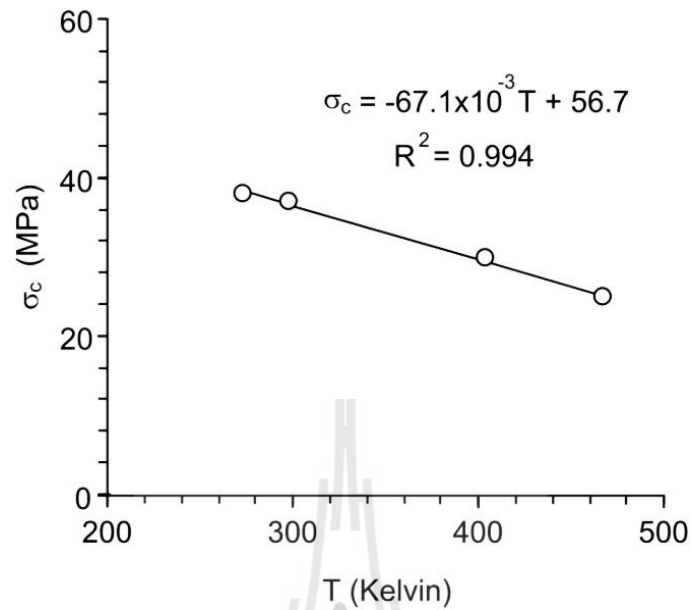
Figure 5.1 Uniaxial compressive strength of salt as a function of temperature. The temperature varies from 277, 298, 394 to 456 Kelvin

Table 5.1 Uniaxial compressive strengths of salt.

Specimen no.	Density, ρ (g/cc)	Temperature (Kelvin)	σ_c (MPa)
UCS 45-47	2.12 ± 0.03	277.0 ± 2.3	37.9 ± 3.0
UCS 81,87,90	2.00 ± 0.05	298.0 ± 0.6	37.0 ± 2.5
UCS 51-53	2.10 ± 0.01	394.0 ± 4.7	30.0 ± 3.5
USC 74	2.15	455.5	25

5.3 Triaxial compressive strengths

The results are present in form of stress-strain curves and major principal stress (σ_1) at failure as a function of confining pressure (σ_3). The stress-strain curves for rock salt are shown in Figures 5.2 through 5.5. They are obtained from
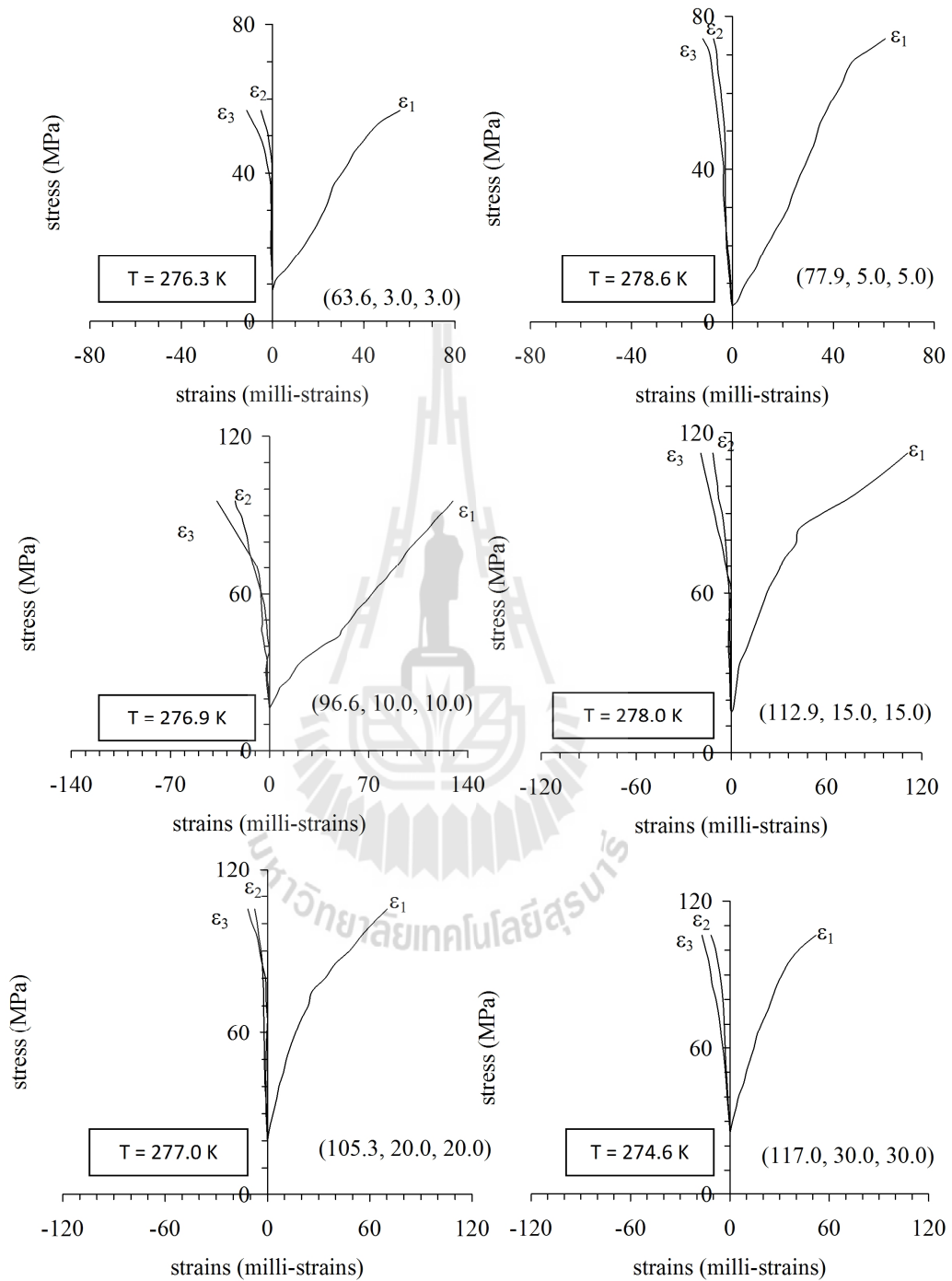
Figure 5.2 Stress-strain curves obtained from some salt specimens under 277.0 ± 2.3 Kelvin. Numbers in brackets indicate ($\sigma_1, \sigma_2, \sigma_3$) at failure.
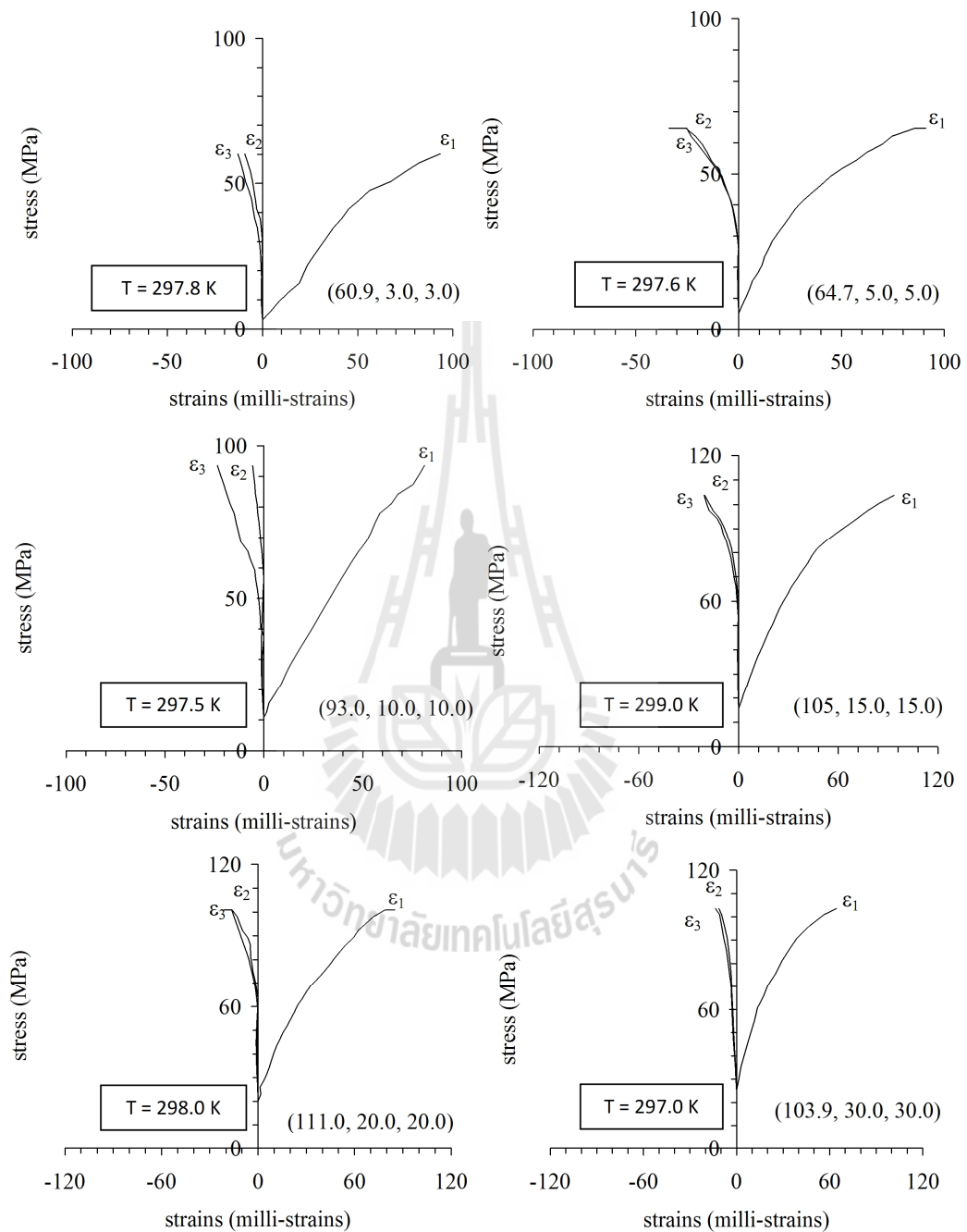
Figure 5.3   Stress-strain curves obtained from some salt specimens under $298.0 \pm$

0.6 Kelvin. Numbers in brackets indicate $(\sigma_1, \sigma_2, \sigma_3)$ at failure.
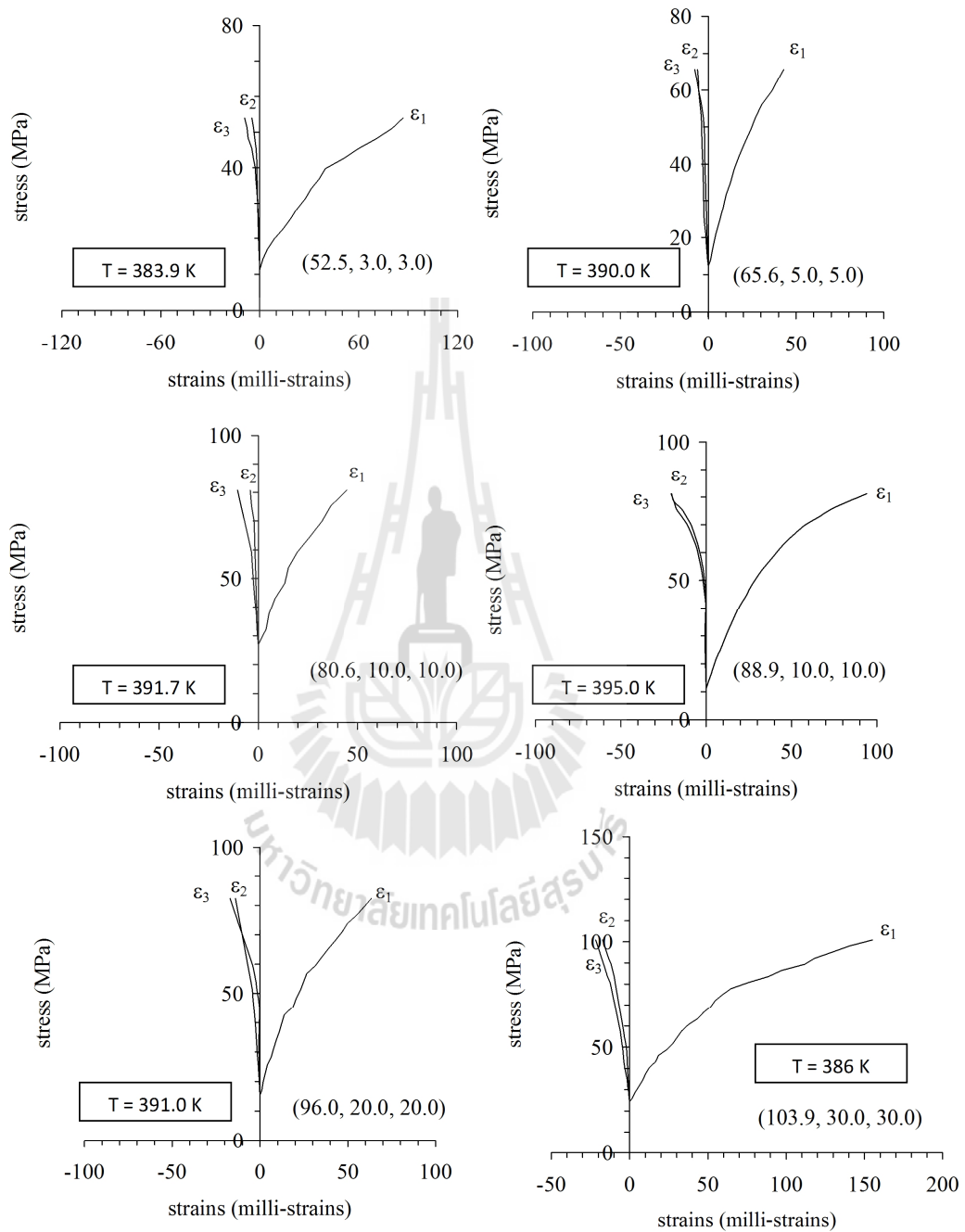
Figure 5.4 Stress-strain curves obtained from some salt specimens under 394.0 ±

4.7 Kelvin. Numbers in brackets indicate $(\sigma_1, \sigma_2, \sigma_3)$ at failure.
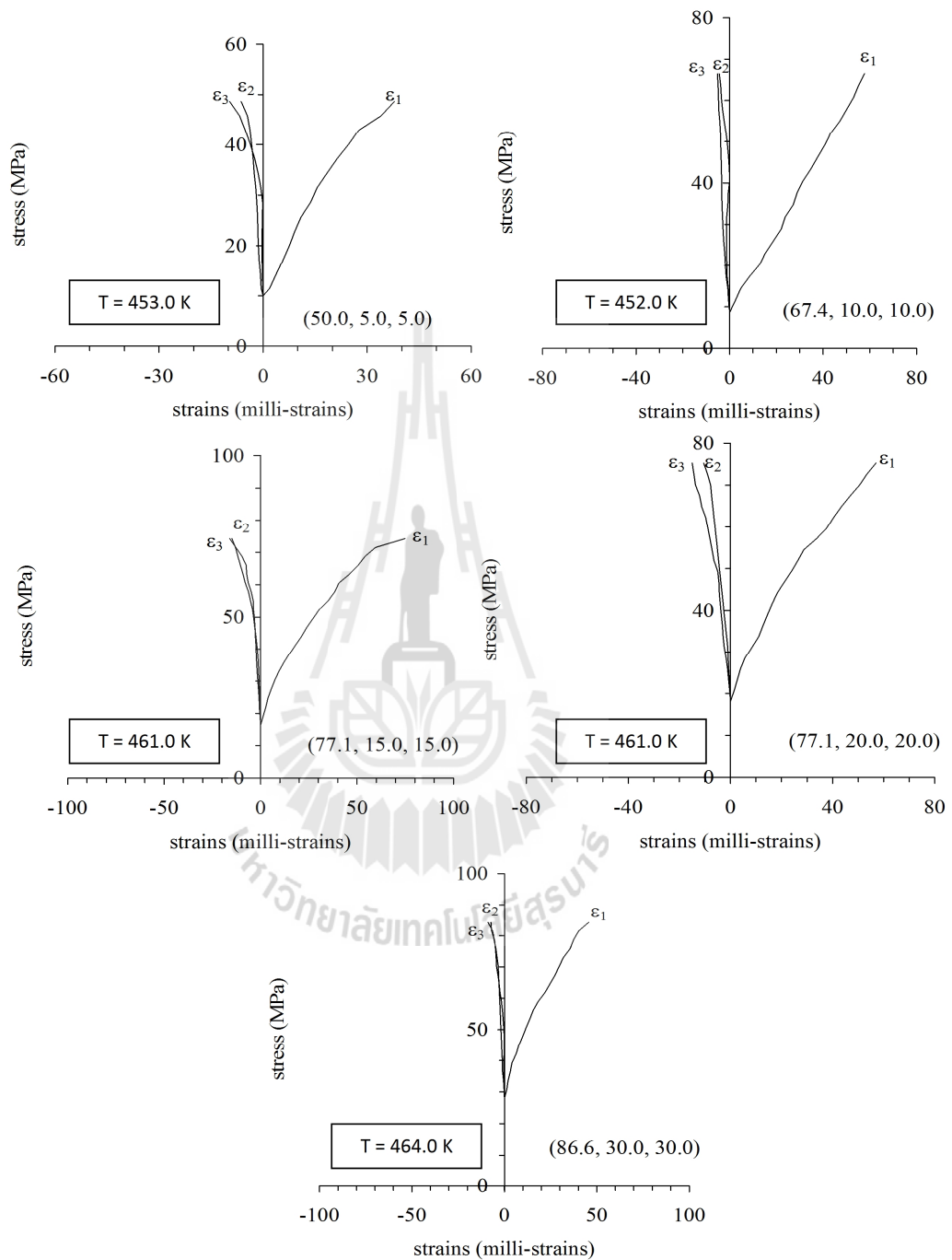
Figure 5.5   Stress-strain curves obtained from some salt specimens under 458.2 ± 4.8

Kelvin.   Numbers in brackets indicate $(\sigma_1, \sigma_2, \sigma_3)$ at failure.

the salt specimens under various temperatures and confining pressures. For all specimens the two measured lateral strains induced by the same magnitude of the applied lateral stresses are similar. Some discrepancies may be due to the intrinsic variability of the salt. The effects of temperature under strength tend to pronounce more under larger confining pressures. This is suggested by that the high temperature increases the salt strain at failure larger than that under lower temperature. Table 5.2 shows the triaxial compressive strength results.

Non-linear behavior of the major principal stress and minor principal stress relations under various temperatures are shown in Figure 5.6. Under the same confining pressure (σ_3) the maximum principal stress at failure (σ_1) decreases with increasing specimen temperature.

Table 5.2 Triaxial compressive strengths of salt.

σ_3 (MPa)	σ_1 (MPa)			
	Testing Temperature			
	274 K	298 K	390 K	467 K
1.6	49.0	45.9	-	-
3	63.6	60.9	52.5	-
5	77.9	76.8	65.6	50.0
10	96.6	93.0	80.6	67.4
15	109.5	105.0	88.9	77.1
20	118.6	113.3	96.0	83.9
30	135.0	128.5	111.0	97.1
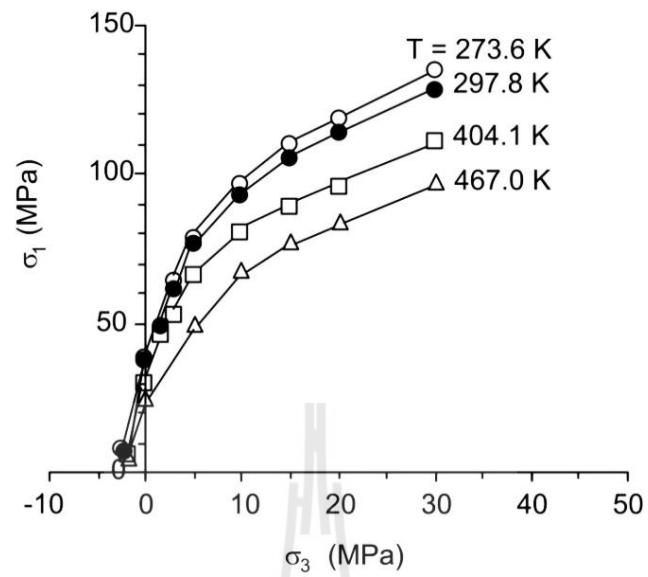
Figure 5.6 Major principal stresses at failure as a function of confining pressure.
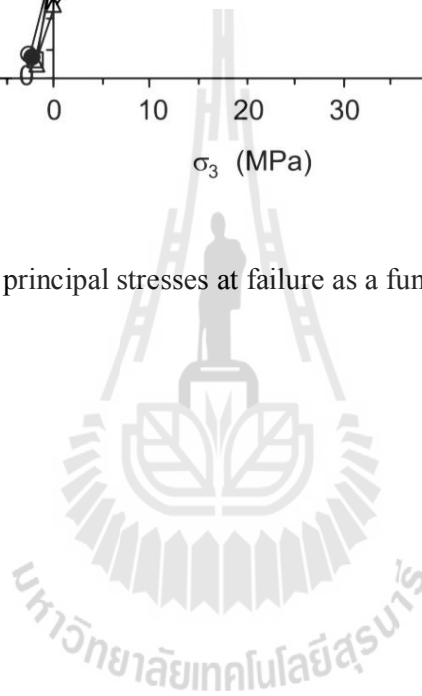
5.4 Brazilian tensile strength test results

Table 5.3 shows the test results. The tensile strength (σ_B) decreases linearly with increasing specimen temperature (T), and can be represented by:

$$\sigma_B = -12 \times 10^{-3}T + 10.5 \text{ MPa} \qquad ;T(\text{Kelvin}) \qquad (5.2)$$

The maximum principal stresses at failure (σ_1) from the compressive and tensile testing can be presented as a function of the minimum principal stress (σ_3) in Figure 5.7. Non-linear relations can be observed at all temperature levels. The higher temperature imposed on the salt specimen, the lower failure envelope is obtained.

Table 5.3 Brazilian tensile strengths of salt.

Specimen no.	ρ (g/cc)	Temperature (Kelvin)	σ_B (MPa)
BZ 1-10	2.12 ± 0.01	274.0 ± 3.1	7.3 ± 0.51
BZ 11-20	2.10 ± 0.05	297.5 ± 0.8	6.0 ± 0.60
BZ 21-30	2.21 ± 0.04	393.7 ± 5.1	5.8 ± 0.84
BZ 31-40	2.09 ± 0.04	464.7 ± 4.5	4.8 ± 0.42

5.5 Mechanical static loading test results

For this series the static loading are subjected to the salt specimen with a cylindrical core 100 mm in diameter. The constant axial stresses range from 6.5 to 16 MPa and temperatures from 300 to 373 Kelvin. The vertical and lateral displacements are monitored. The results are presented in form of the axial strain-time and lateral strain-time curves. The strain-time curves (ε-t) for the static loading with constant axial stress ranging from 6.5 to 16 MPa are shown in Figures 5.8 and 5.9.
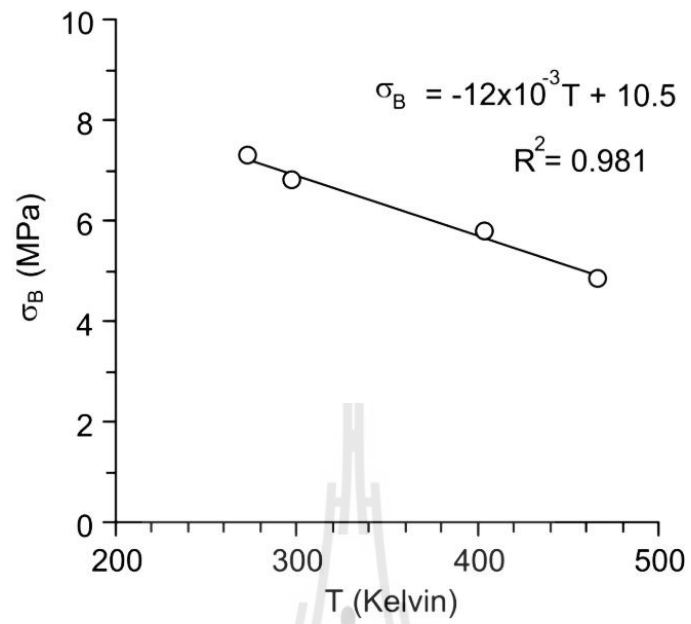
Figure 5.7   Brazilian tensile strength of salt as a function of temperature.
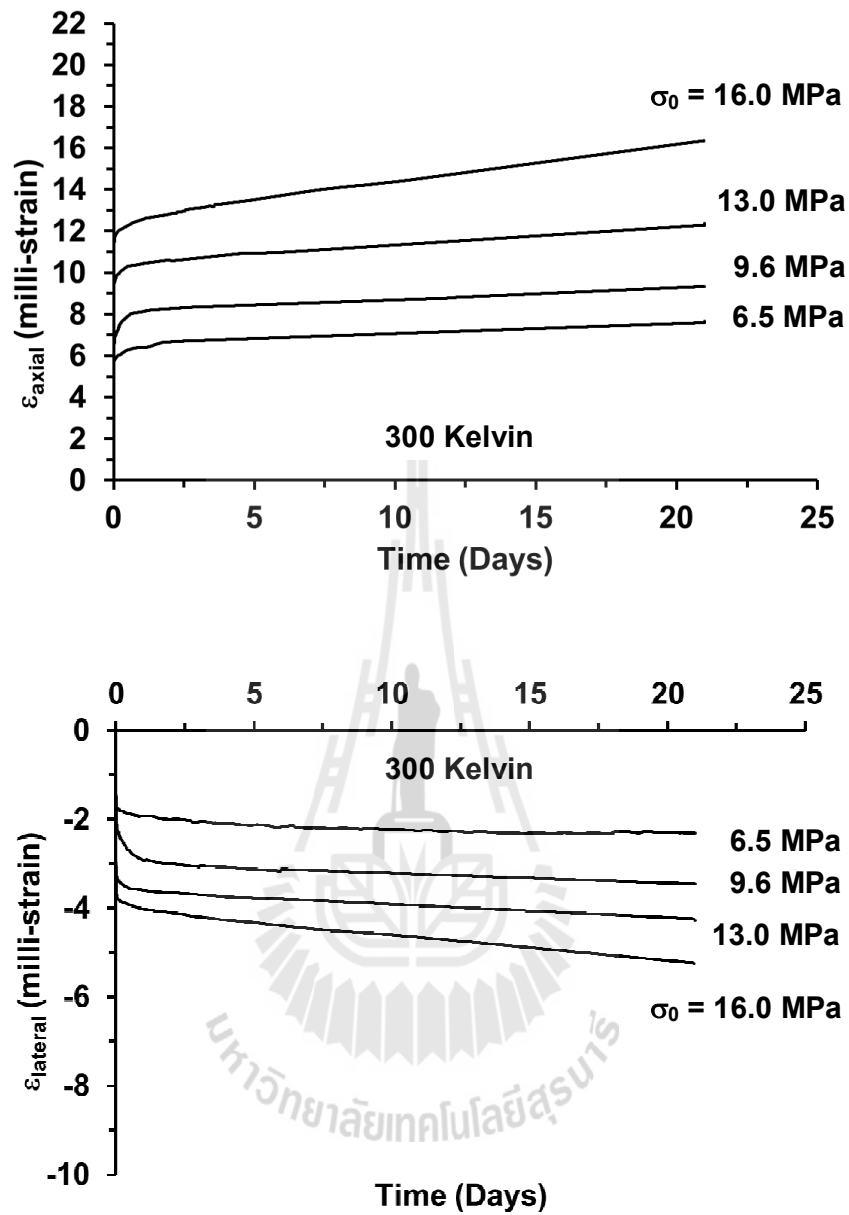
Figure 5.8 Axial and lateral strains (ε_{axial}, ε_{lat}) as a function of time (t) for static loading under maximum axial stresses of 6.5, 9.6, 13, and 16 MPa at room temperature (300 K).
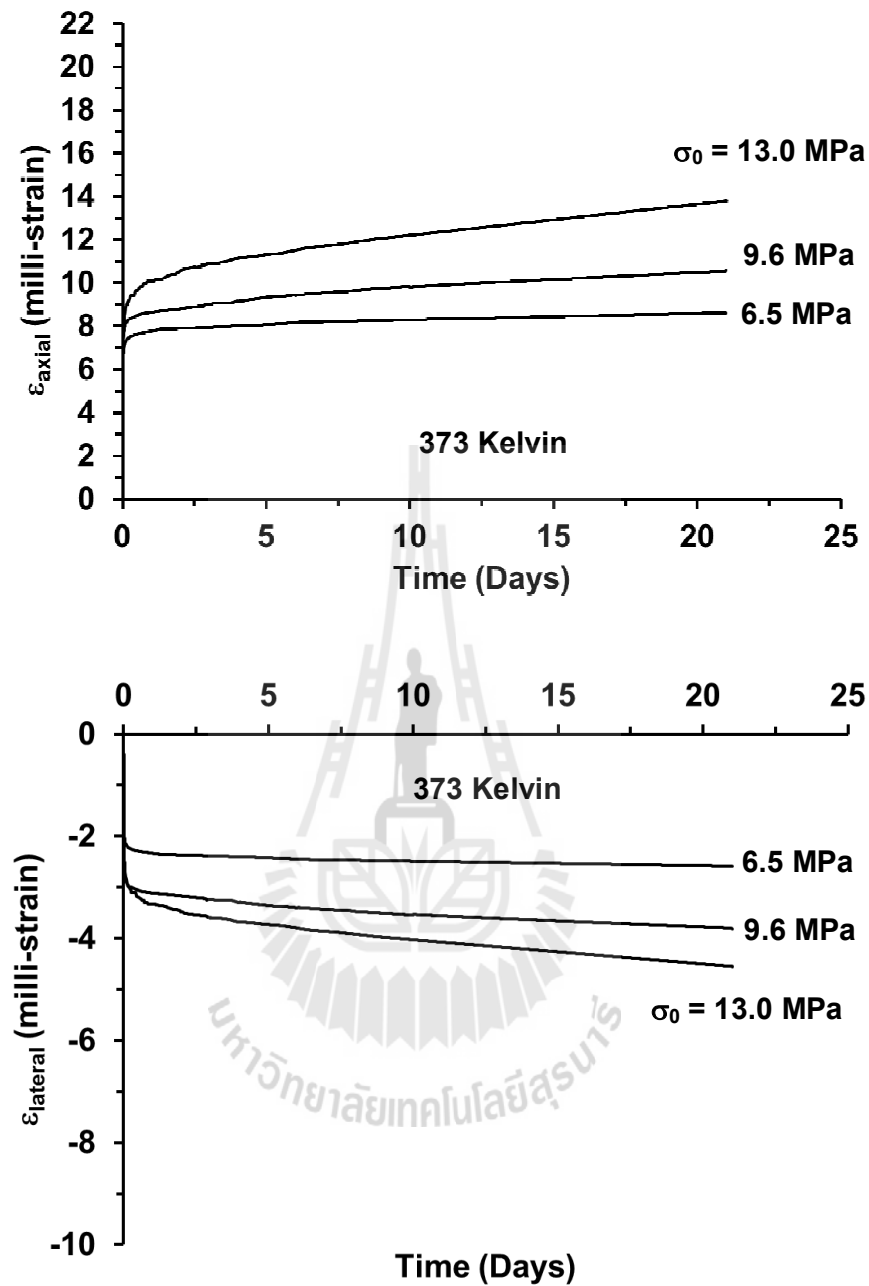
Figure 5.9 Axial and lateral strains (ε_{axial}, ε_{lat}) as a function of time (t) for static

loading under maximum axial stresses of 6.5, 9.6 and 13 MPa at high

temperature (373 K).

Each salt specimen shows instantaneous, transient creep phase and steady-state creep phase. The salt specimens continue to deform without failure. The temperature can be increased the creep deformation particularly, under high axial stresses.

5.6   Mechanical cyclic loading test results

This test series the cyclic loading have been performed on the same specimens which tested on the static loading after the results are recorded for 21 days. After 21 days under MSL testing the salt specimens are unloaded to the minimum stress of 1 MPa for 12 hours and reloaded to the selected axial stress for each specimen for 12 hours. The results are presented in form of the axial strain-time and lateral strain-time curves. The strain-time curves for the cyclic loading with constant axial stress range from 6.5 to 16 MPa are shown in Figures 5.10 and 5.11. Under mechanical cyclic loading, the instantaneous, transient and steady-state phase still are observed in each cycle. For the applied axial stress under unloaded condition at 1 MPa, the axial strain decreases. When the specimens are subjected to cyclic loading slightly higher creep strains are observed at all stress levels for both room and elevated temperature. These are observed for both axial and lateral strains on the salt samples.

The strain of specimens increase by about 23.2% to 34.4% after the loading changes from static to cyclic phases under room and elevated temperature, respectively.
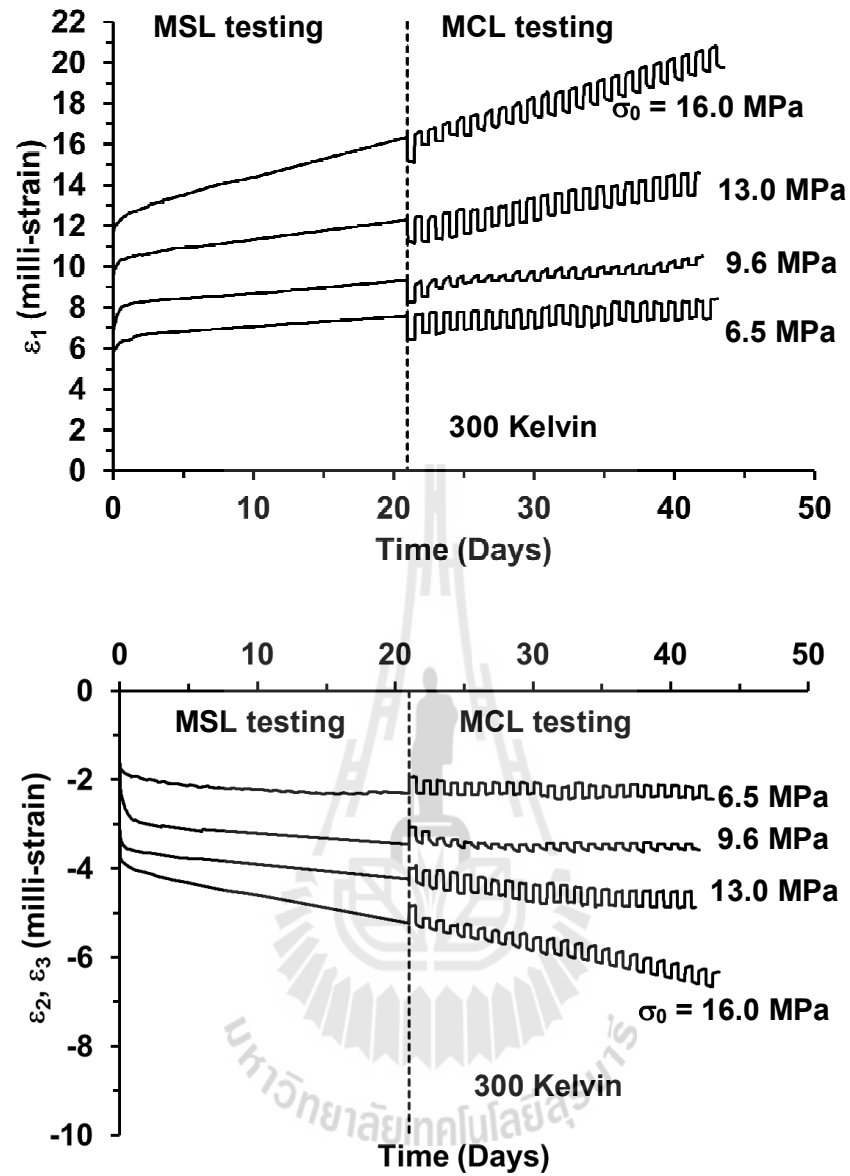
Figure 5.10 Axial and lateral strains (ε_{axial}, ε_{lat}) as a function of time (t) for static and cyclic loading under maximum axial stresses of 6.5, 9.6, 13, and 16 MPa at room temperature (300 K).
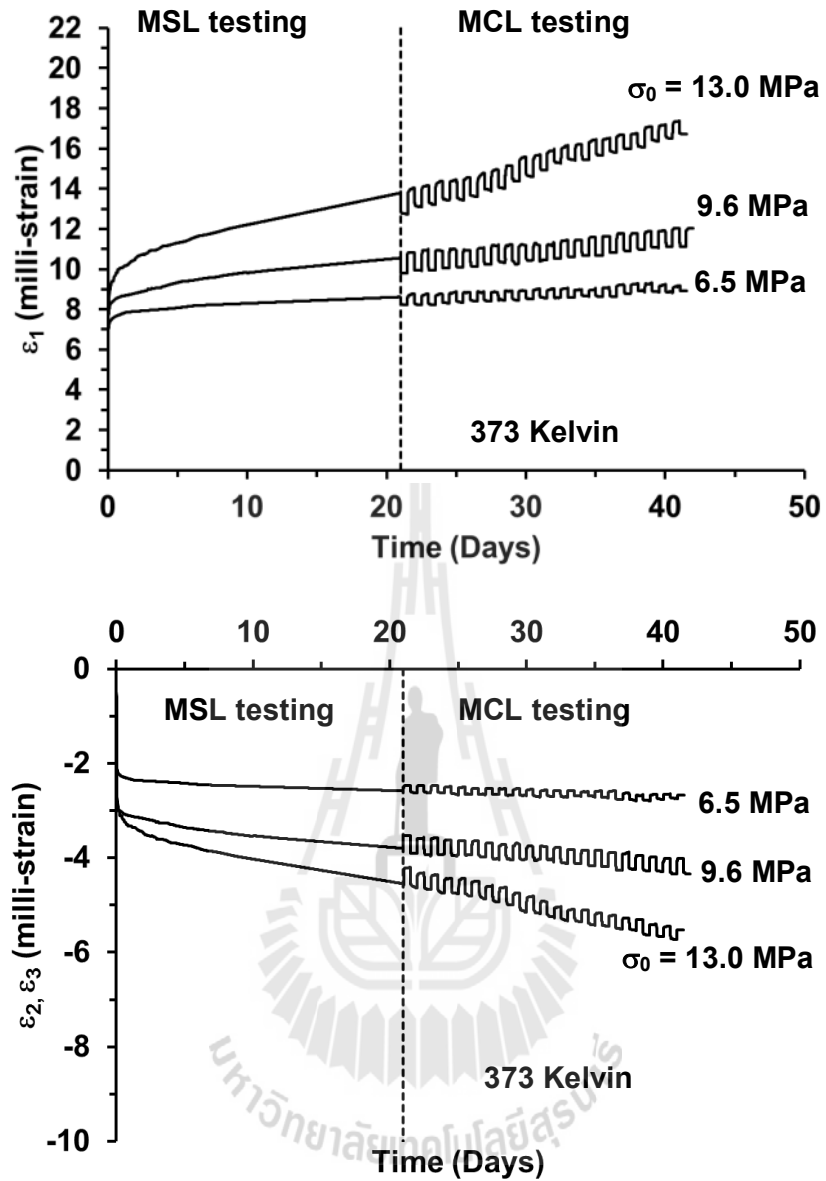
Figure 5.11 Axial and lateral strains (ε_{axial}, ε_{lat}) as a function of time (t) for static and cyclic loading under maximum axial stresses of 6.5, 9.6, 13, and 16 MPa at high temperature (373 K).

5.7   MTCL test results

The MTCL tests are performed by combining the effects of cyclic thermal and mechanical loadings. This test series were used the other rock salt samples which tested on static loading condition.   After the static loading under ambient temperature for 21 days, the salt specimens are unloaded to the minimum stress of 1 MPa under 373 K for 12 hours and reloaded to the selected axial stress under 300 K for 12 hours. The thermal and mechanical cyclic loading period is 21 days.

For MTCL tests, the axial creep strains are highest compared to the other two conditions.   When the specimens are subjected to cyclic phase, the highest creep strains are observed at 36.4%.   The amplitude for each cycle is affected by temperature which clearly observed in the MTCL testing.   Figure 5.12 shows the strains as a function of the time for the MTCL testing.

5.8   Discussions of the test results

The salt strengths under different constant temperatures are observed.   For each temperature level the testing is assumed to be under isothermal condition (constant temperature with time during loading). The decrease of the salt strength as the temperature increases suggest that the applied thermal energy before the mechanical testing makes the salt weaker, and more plastic – failing at lower stress and higher strain with lower elastic and shear moduli. The temperature effect is larger when salt is under higher mean stress.
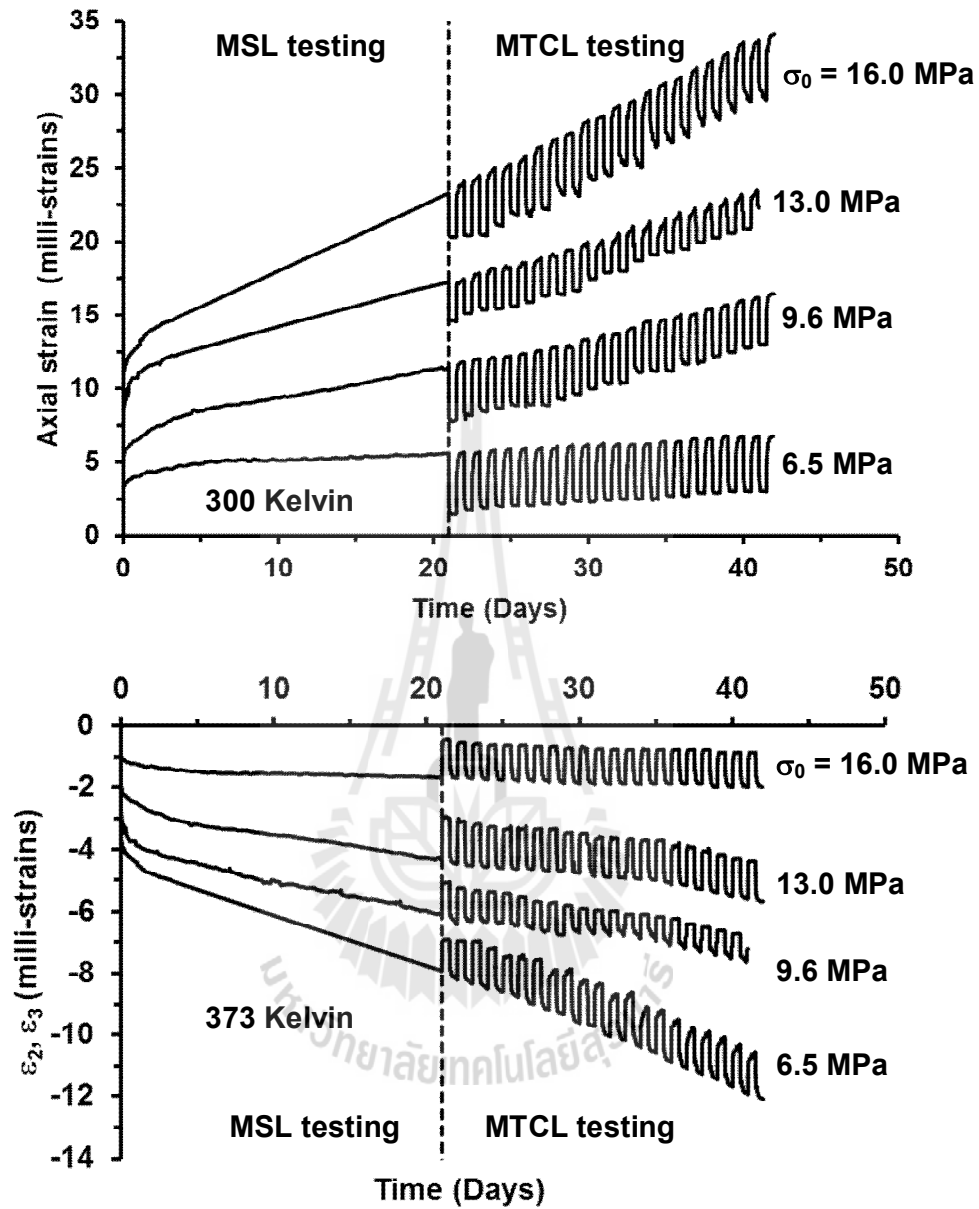
Figure 5.12 Axial and lateral strains (ε_{axial}, ε_{lat}) as a function of time (t) for mechanical and thermal cyclic loading under maximum axial stresses of 6.5, 9.6, 13, and 16 MPa.

For the conventional uniaxial creep under room and high temperature, the results indicate that the differences of temperature on the specimens have affected the octahedral shear strains in each condition. They are increased when the temperature increases, particularly under high axial stresses. When the specimens are subjected to cyclic loading slightly higher creep strains are observed at all stress levels for both room and elevated temperatures. This is because the amplitude (or range) of the cyclic stress that can be applied to the specimens without causing failure. The effect of cyclic stresses may operate indefinitely a crack growth when loads in each cycle. This indicates that the specimens can absorb the stress and crack propagation that are occurred. The amplitude obtained from the MTCL specimens tends to be higher than those under mechanical cyclic loading, which suggests that the cyclic thermal loading has significant effect on the salt deformation.
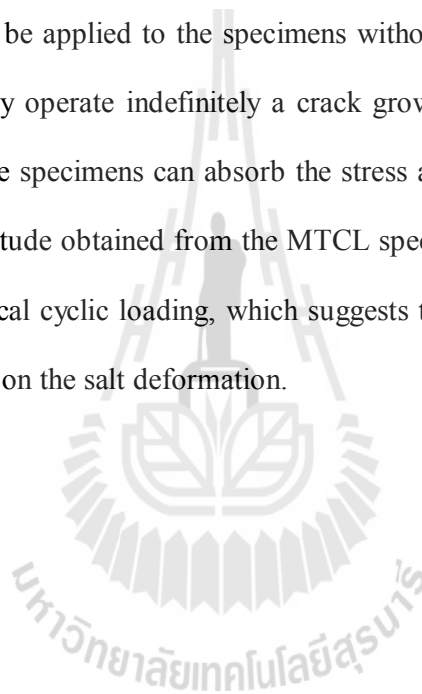
CHAPTER VII

DISCUSSIONS, CONCLUSIONS, AND

RECOMMENDATIONS FOR FUTURE STUDIES

7.1   Discussions

This section discusses the key issues relevant to the reliability of the test results and adequacies of the test specimens to reach conclusion. Suitability of the Burgers model, the accuracy of the monitoring and temperature-controlled system are described. Comparisons of the MCL and MTCL test from this study which can be representative to the actual condition of the storage cavern have also been made.

The conventional creep tests by using the consolidation or polyaxial load frame have been used by several researches (Sriapai et al., 2011; Fuenkajorn et al., 2012; Samsri et al., 2011). As evidenced by the good fitting obtained from the Burgers model, the test results are believed to be reliable. This is true for all test series.

The measurement systems use the dial gauge to monitor the specimen deformation with accuracy of ±0.01 mm. It can however use the other method such as optical or laser system but the specimens used here is rock salt which it is transparent material as a result the above system may not be applicable. The temperature-controlled systems used here can be adjustable and controllable to the nearest ±5 degrees of Celsius. The test period is 21 days for static loading and 21 days for MCL and MTCL loading which is sufficient for the creep deformation measurement in the

transient through the steady-state phase.

In the actual storage, the operation scheme of 1 cycle/day (12 hours injection and 12 hours withdrawal) gives the lowest factor of safety (Fuenkajorn et al., 2012). The cyclic frequencies used here is suitable and comparable with the compressed-air energy storage at gas injection-withdrawal period of 1 cycle/day which is highest rate possible. The actual frequencies of the gas injection-withdrawal are likely slower than the rates used here which can provide lower closure rate than that obtained from this study.

The MTCL method can be representative of the actual compressed-air storage because the caverns under the actual storage condition is subject to high internal pressure or low octahedral shear stress the high temperature when is subjected to the injection period. On the other hand, the cavern under low internal pressure or high octahedral shear stress will be subjected to the low temperature. The results obtained here provide the maximum cavern closure and maximum closure rate based on the mechanical and thermal cyclic loading test condition. The amplitude obtained from the MTCL specimens tend to be higher than those under mechanical cyclic loading that because of the effect of temperature.

7.2 Conclusions

All objectives and requirements of this study have been met. The results of the laboratory testing and analyses can be concluded as follows:

(1) The effect of temperature can be observed from the relations of the uniaxial compressive strength of salt as a function of temperature (Figure 5.2). It can reduce the salt strength, particularly under high temperature, and tends to decrease when the

temperature are increased.   The decrease of the salt strength as the temperature increases suggest that the applied thermal energy before the mechanical testing makes the salt weaker, and more plastic – failing at lower stress and higher strain with lower elastic and shear moduli. The temperature effect is larger when salt is under higher mean stress.

(2) The temperature effect can be observed more clearly from stress-strain curves and σ_1-σ_3 diagrams.   The salt strains are increased under larger confining pressures.   Under the same confining pressure (σ_3) the maximum principal stress at failure (σ_1) decreases with increasing specimen temperature.

(3) The tensile strength of the salt under various temperatures has been observed from Brazilian tensile strength test.   The tensile strength decreases linearly with increasing specimen temperature (see Figure 5.7).

(4) Conventional creep test or mechanical static loading (MSL) under room and high temperatures can be observed from strain-time curves.   The results indicate that the differences of temperature on the specimens have affected the octahedral shear strains and creep deformation under each condition.   They are increased when the temperature increases, particularly under high axial stresses.

(5) Mechanical cyclic loading (MCL) performed here has advantages over the mechanical static loading tests.   It allows simulating the behavior of the salt creep deformation rate under cavern fluctuation of compressed-air storage.   When the specimens are subjected to cyclic loading slightly higher creep strains are observed at all stress levels for both room and elevated temperatures.

(6) The mechanical and thermal cyclic testing technique performed here has clearly demonstrated the behavior of salt cavern under gas injection and withdrawal

period. The axial creep strains are highest compared to the other two conditions. The amplitude for each cycle is affected by temperature which is greater than that of the MCL testing.

(7) The calibration of the steady-state creep phase can be represented by the Burger model. The creep strain magnitude and rate under cyclic loading is slightly higher than under static loading under elevated temperature (about 23.2% to 34.4%). The stress and temperature cycles induce a higher creep strain than do the static loading for all applied stress levels.

(8) The visco-plastic parameters (η_1) calibrated from the test results are used in the simulations of the creep deformation of compress-air storage caverns by using FLAC and creep equations. From the results from creep equation, the cavern closure rates under MSL testing are 19.7 and 21.5 % per month for ambient and elevated temperature, and under the MCL testing are 21.3 and 23.6 % per month for ambient and elevated temperature. The maximum closure rate under mechanical and thermal loading is about 33.7 % per month.

The FLAC results indicate that, the cavern closure rate under MSL testing is about 11.7 and 12.9 % per month for ambient and elevated temperature, the MCL testing the closure rate is about 13.0 and 14.7 % per month for ambient and elevated temperature, and 24.8 % per month for MTCL testing. The results from equation give the higher closure and closure rate than those from the FLAC simulations.

The results suggest that the property parameters obtained from the MSL test can under-estimate the cavern deformation when it subjects to cavern pressure fluctuation, as evidenced by the MCL or MTCL tests. This implies that the results from the conventional uniaxial creep testing could lead to a non-conservative design

and stability analysis for the salt caverns that subject to injection and retrieval of the stored products. For a simplified practice, the visco-plastic parameters should be adjusted by about 29% - 38% for the conventional test results for conservative design.

7.3   Recommendations for future studies

Recognizing that the numbers of the specimens and the test parameters used here are limited, more testing and measurements are recommended, as follows:

(1) Increasing the number of the specimens would enhance the reliability of the test results and accessibility of the creep deformation or cavern closure of the rock salt compressed-air energy storage.

(2) The effects confining pressure should be investigated. In this study the confining pressure is zero which may not sufficient to predict creep deformation around salt solution cavern. In generally, the salt around a cylindrical cavern is under polyaxial stress state ($\sigma_\theta > \sigma_z > \sigma_r$). Hence, for more realistic it should be noted that the static and cyclic loading test under multi-axial stresses including the mechanical and thermal cyclic loading testing technique used here are desirable for this task.

(3) Different loading frequencies should be performed to compare with the other injection-withdrawal period. Because of the number of cycles may affect to crack growth in the specimen, higher number of loading cycles should be used.

(4) Different loading amplitudes should be performed. Lower amplitude testing is desirable. This should provide the strain-time curves that are close to the actual condition.

REFERENCES

Allemandou, X. and Dusseault, M.B. (1996). Procedures for cyclic creep testing of salt rock, results and discussions. In **Proceedings of the Third Conference on the Mechanical Behavior of Salt** (pp. 207-218). Clausthal-Zellerfeld, Germany: Trans Tech Publications.

ASTM D2664. Standard test method for triaxial compressive strength of undrained rock core specimens without pore pressure measurements. In **Annual Book of ASTM Standards** (Vol. 04.08). Philadelphia: American Society for Testing and Materials.

ASTM D2938. Standard test method for unconfined compressive strength of intact rock core specimens. In **Annual Book of ASTM Standards** (Vol. 04.08). Philadelphia: American Society for Testing and Materials.

ASTM D3967. Standard test method for splitting tensile strength of intact rock core specimens. In **Annual Book of ASTM Standards** (Vol. 04.08). Philadelphia: American Society for Testing and Materials.

ASTM D4405. Standard test method for creep of cylindrical soft rock core specimens in uniaxial compressions. In **Annual Book of ASTM Standards** (Vol. 04.08). Philadelphia: American Society for Testing and Materials.

ASTM D4543. Standard practice for preparing rock core specimens and determining dimensional and shape tolerances. In **Annual Book of ASTM Standards** (Vol. 04.08). Philadelphia: American Society for Testing and Materials.

ASTM D7070-08. Creep of rock core under constant stress and temperature. **Annual Book of ASTM Standards**, 04.08, ASTM International, West Conshohocken, PA.

Aubertin, M. (1996). On the physical origin and modeling of kinematics and isotropic hardening of salt. In **Proceedings of the Third Conference on the Mechanical Behavior of Salt** (pp. 1-18). Clausthal-Zellerfeld, Germany: Trans Tech Publications.

Bagde, M.N. & Petros, V. (2005). Fatigue properties of intact sandstone samples subjected to dynamic uniaxial cyclical loading. **International Journal of Rock Mechanics and Mining Sciences**, 42(2): 237-250.

Bauer, S., Broome, S., Bronowski, D., Rinehart, A., Ingraham M.D. (2011). Experimental deformation of salt in cyclic loading, insights from acoustic emission measurements. **Solution Mining Research Institute Spring 2011 Technical Conference Galveston**, Texas, USA, April 2011, pp. 1-16.

Cleach, J.M.L., Ghazali, A., Deveughele, H., and Brulhet, J. (1996). Experimental study of the role of humidity on the thermomechanical behavior of various halitic rocks. In **Proceedings of the Third Conference on the Mechanical Behavior of Salt** (pp. 231-236). Clausthal-Zellerfeld, Germany: Trans Tech Publications.

Cristescu, N. and Hunsche, U. (1996). A comprehensive constitutive equation for rock salt determination and application. In **Proceedings of the Third Conference on the Mechanical Behavior of Salt** (pp. 191-205). Clausthal-Zellerfeld, Germany: Trans Tech Publications.

Dusseault, M.B. and Fordham, C.J. (1993). Time-dependent behavior of rocks. **Comprehensive Rock Engineering Principles, Practice and Project: Rock Testing and Site Characterization** (Vol. 3, pp. 119-149). London, Pergamon.

Dwivedi, R.D., Goel, R.K., Prasada, V.V.R. and Sinhab, A. (2008). Thermo-mechanical properties of Indian and other granites. **International Journal of Rock Mechanics and Mining Sciences** 45 (2008): 303-315.

Farmer, I.W. and Gilbert, M.J. (1984). Time dependent strength reduction of rock salt. In **Proceedings of the First Conference on the Mechanical Behavior of Salt** (pp. 3-18). Clausthal-Zellerfeld, Germany: Trans Tech Publications.

Findley, W.N., Lai, J.S., Onaran, K. (1989). **Creep and Relaxation of Nonlinear Viscoelastic Material: With an Introduction to Linear Viscoelasticity**. North-Holland, New York. 371 pp

Fokker, P. A. (1998). The micro-mechanics of creep in rock salt. In **Proceedings of the Fourth Conference on the Mechanical Behavior of Salt** (pp. 49-61). Clausthal-Zellerfeld, Germany: Trans Tech Publications.

Franssen, R.C.M. and Spiers, C.J. (1990). Deformation of polycrystalline salt in compression and in shear at 250-350°C. Deformation Mechanisms, Rheology and Tectonics, **Geological Society Special Publication** (Vol. 45, pp. 201-213).

Fuenkajorn, K, Sriapai, T., and Samsri, P. (2012). Effects of loading rate on strength and deformability of Maha Sarakham salt. **Engineering Geology**, 135-136(2012): 10-23.

Fuenkajorn, K. and Daemen, J. J. K. (1988). **Boreholes closure in salt**. Technical Report Prepared for The U.S. Nuclear Regulatory Commission. Report No. NUREG/CR-5243 RW. University of Arizona.

Fuenkajorn, K. and Phueakphum, D. (2010). Effects of cyclic loading on mechanical properties of Maha Sarakham salt. **Engineering Geology**. 112 (1-4) 43-52.

Fuenkajorn, K., Walsri, C., and P hueakphum, D. (2011). Intrinsic variability of the mechanical properties of Maha Sarakham salt. **Quarterly Journal of Engineering Geology and Hydrogeology** 44 : 445-456.

Furong, T., Xianbiao, M., Lianying, Z., Huiguang, Y., and Yan, L. (2011). Effects of strain rates on mechanical properties of limestone under high temperature. **Mining Science and Technology (China)** 21: 857–861.

Haimson, B.C. (1974). Mechanical behavior of rock under cyclic loading. In **Proceedings of the 3rd Congress of the International Society for Rock Mechanics, Part A. Advances in Rock Mechanics: Report of Current Research, 1-7 September**. National Academy of Sciences: Washington, D.C., pp. 373-387.

Hamami, M., Tijani, S.M., and Vouille, G. (1996). A methodology for the identification of rock salt behavior using multi-step creep tests. In **Proceedings of the Third Conference on the Mechanical Behavior of Salt** (pp. 53-66). Clausthal-Zellerfeld, Germany: Trans Tech Publications.

Hunsche, U. and Schulze, O. (1996). Effect of humidity and confining pressure on creep of rock salt. In **Mechanical Behavior of salt, Series on Soil and Rock Mechanics** (Vol. 20, pp. 237-248). Trans Tech Publications.

Inada, Y., Kinoshita, N., Ebisawa, A., and Gomi, S. (1997). Strength and deformation characteristics of rocks after undergoing thermal hysteresis of high and low temperatures. **International Journal of Rock Mechanics and Mining Sciences** 34 (3-4): 688-702.

Itasca (1992). **User Manual for FLAC-Fast Langrangian Analysis of Continua, Version 4.0**. Itasca Consulting Group Inc. Minneapolis, Minnesota.

Jaeger, J.C., Cook, N.G.W., and Zimmerman, R.W. (2007). **Fundamentals of Rock Mechanics**. Chapman and Hall, London, 474 p.

Jeremic, M. L. (1994). **Rock mechanics in salt mining** (530 pp.). Rotherdam: A. A. Balkema.

Kensakoo, T. (2006). Relationship between mineralogy and engineering properties of rock salt. M.S. Thesis, Suranaree University of Tehnolgy, Thailand.

Kodama, J., Ishizuka, Y., Abe, T., Ishijima, Y. & Goto, T. (2000). Estimate of the fatigue strength of granite subjected to long-period cyclic loading. **Shigen-to-Sozai**, 116: 111-118.

Liang, W.G., Xu, S.G., and Zhao, Y.S. (2006). Experimental study of temperature effects on physical and mechanical characteristics of salt rock, **Rock Mechanics and Rock Engineering**. 39(5): 469-482.

Obert, L. and Duvall, W. I. 1967. Rock mechanics and the design of structures in rock. **Journal of the Franklin Institute**. New York.

Okatov, R.P., Nizametdinov, F.K. Tsai, B.N., and Bondarenko, T.T. (2003). Time and temperature factors in construction of rock strength criteria, **Journal of Mining Science.** 39(2): 139-142.

Pudewills, A. and DrostePapp, J. (2003). Numerical modeling of the thermomechanical behavior of a large-scale underground experiment. **Computers & Structures** (81 (2003): 911-918).

Pudewills, A., Muller-Hoeppe, N. and Papp, R. (1995). Thermal and thermomechanical analyses for disposal in drifts of a repository in rock salt. **Nuclear Technology** 1: 79-88.

Raj, S.V. and Pharr, G.M. (1992). Effect of temperature on the formation of creep substructure in sodium chloride single crystal. **American Ceramic Society** 75 (2): 347-352.

Ray, S.K., Sarkar, M. and Singh, T.N. (1999). Effect of cyclic loading and strain rate on the mechanical behaviour of sandstone. **International Journal of Rock Mechanics and Mining Sciences**, 36(4): 543-549.

Samsri, P., Sriapai, T., Walsri ,C. and Fuenkajorn, K. (2011). Polyaxial creep testing of rock salt. In **Proceedings of the Third Thailand Symposium on Rock Mechanicson** (pp. 125-132). Thailand.

Senseny, P. E. (1983). **Review of constitutive laws used to describe the creep of salt.** Battelle Memorial Institute. Columbus.

Senseny, P.E., Handin, J.W., Hansen, F.D., and Russell, J.E. (1992). Mechanical behavior of rock salt: phenomenology and micro-mechanisms. **International Journal of Rock Mechanics and Mining Sciences** 29 (4): 363-378.

Shimada, M. & Liu, J. (2000). Temperature dependence of strength of rock under high confining pressure, **Annuals of Disas**., Prev. Res. Inst. No. 43B-1, pp. 75-84.

Singh, T.N., Ray, S.K. & Singh, D.P. (1994). Effect of uniaxial cyclic compression on the mechanical behaviour of rocks. **Indian Journal of Engineering & Materials Sciences**, 1(2): 118-120.

Sriapai, T., Samsri, P. and Fuenkajorn, K. (2011). Influence of loading rate on compressive strength of rock salt. In **Proceedings of the Third Thailand Symposium on Rock Mechanicson** (pp. 117-124). Thailand.

Sriapai, T., Walsri, C. and Fuenkajorn, K. (2012). Effect of temperature on compressive and tensile strengths of salt. **ScienceAsia,** 38(2): 166-174.

Vosteen, H. & Schellschmidt, R. (2003). Influence of temperature on thermal conductivity, thermal capacity and thermal diffusivity for different types of rock, **Physics and Chemistry of the Earth**. Parts A/B/C, 28: 499-509.

Wanten, P.H., Spiers, C.J., and Peach, C.J. (1996). Deformation of NaCl single crystals at $0.27Tm < T < 0.44Tm$. In **Proceedings of the Third Conference on the Mechanical Behavior of Salt** (pp. 117-128). Clausthal-Zellerfeld, Germany: Trans Tech Publications.

Warren, J. (1999). **Evaporites: Their evolution and economics** (pp. 235-239). Philadelphia: Blackwell Science.

Wendai, L. (2000). Regression analysis, liner regression and probit regression In 13 chapters**. SPSS for Windows: statistical analysis**. Publishing House of Electronics Industry. Beijing.

Yang, C. and Daemen, J. J. K. (1997). Temperature effects on creep of tuff and its time-dependent damage analysis. **International Journal of Rock Mechanics and Mining Sciences** 34 (3-4): 383-395.

Yavuz, H., Demirdag, S., and Caran, S. (2010). Thermal effect on the physical properties of carbonate rocks. **International Journal of Rock Mechanics and Mining Sciences** 47: 94-103.

Zhenyu, T. and Haihong, M. (1990). An experimental study and analysis of the behaviour of rock under cyclic loading**. International Journal of Rock Mechanics & Mining Sciences**, 27(1): 51-56.
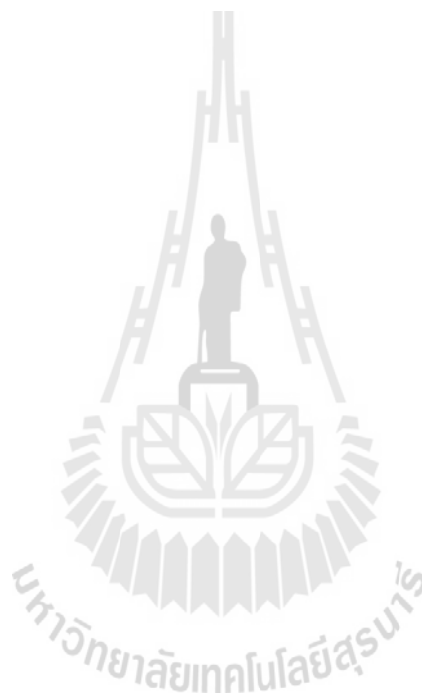
APPENDIX A

DEVELOPMENT A FORMULAE

OF CYLINDRICAL CAVERN CLOSURE

The purpose of this section is to develop analytical solutions to calculate radial and tangential displacements around a circular hole in an infinite plate of linear viscoelastic material subjected to a biaxial lateral stress field. The analysis is performed in plane strain.

The radial displacements around the circular hole obtained from the elastic solution (Obert and Duvall 1967) can be expressed as:

$$u_r = (1 / E) [((\sigma_x + \sigma_y) / 2) \cdot (r + (a^2/r)) + ((\sigma_x - \sigma_y) / 2) \cdot (r - (a^4 / r^3) + (4a^2 / r)) \cdot$$
$$\cos2\theta] - (v / E) [(\sigma_x - \sigma_y) / 2 \cdot (r - (a^2/r)) - ((\sigma_x - \sigma_y) / 2) \cdot$$
$$(r - (a^4 / r^3))\cos2\theta] \tag{A.1}$$

where σ_x, σ_y = lateral stresses, a = hole radius, E = Young's modulus, v = Poisson's ratio, θ = tangential coordinate. Let $\sigma_x = P$ and $\sigma_y = kP$, where P is a time-independent applied stress. Eq. A.1 becomes:

$$u = P/E (A) - Pv/E (B) \tag{A.2}$$

where A and B are time-independent functions of position:

$$A = [((1 + k)/2) \cdot (r + (a^2/r))] + [((1 - k)/2) \cdot (r - (a^4/r^3) + (4a^2/r))]\cos2\theta \tag{A.3}$$

$$B = [((1 + k)/2) \cdot (r - (a^2/r))] - [((1 - k)/2) \cdot (r - (a^4/r^3))]\cos2\theta \tag{A.4}$$

where k = stress ratio (σ_y/σ_x). For the internal pressure term we can use a superposition law and Eq. A.2 becomes:

$$u = P/E \ (A) - Pv/E \ (B) - P_i R/2G \tag{A.5}$$

By taking Laplace transformations of Eq. A.2, they can be expressed in terms of transform variable "s" as follows:

$$\hat{u}(s) = [\hat{P}(s) / \hat{E}(s)] \ (A) - [\hat{P}(s) \cdot \hat{v}(s) / \hat{E}(s)] \ (B) - \hat{P}_i(s) \cdot \hat{R}(s)/2\hat{G}(s) \tag{A.6}$$

Substituting $\hat{P}(s)$ by P/S, $\hat{R}(s)$ by R/S, $\hat{E}(s)$ by $(9K\bar{Q}_1/(\bar{Q}_1 + 6K\bar{P}_1))$, and $\hat{v}(s)$ by $(3K\bar{P}_1 - \bar{Q}_1)/(\bar{Q}_1 + 6K\bar{P}_1)$ and Eq. A.6 becomes:

$$\hat{u}(s) = \{P_o/s \ (A) \ [(\bar{Q}_1 + 6K\bar{P}_1)/9K\bar{Q}_1]\} - \{P_o/s \ (B) \ [(3K\bar{P}_1 - \bar{Q}_1)/ 9K\bar{Q}_1]\}$$
$$- [(P_i R/s) \ (\bar{P}_1/\bar{Q}_1)] \tag{A.7}$$

where time operators of the Burgers model are equal to:

$$\bar{P}_1 = 1 + (\eta_1/E_1 + \eta 1/E_2 + \eta_2/E_2) \cdot s + (\eta_1 \eta_2/E_1 E_2) \cdot s^2 \text{ and}$$

$$\bar{Q}_1 = \eta_2 s + (\eta_1 \eta_2/E_2) \cdot s^2$$

Then performing inverse Laplace transformations, the radial displacements (u) around a circular hole in linear viscoelastic media can be expressed as:

$$u(t) = P_o\{[(1/9K) + (2/3)\alpha](A) - [-(1/9K) + (1/3)\alpha](B) - P_i R\alpha\} \tag{A.8}$$

By rearranging terms of Eq. A.8, they can be expressed in a simple form as:

$$u_r = P_o[(A + B / 9K)+(\alpha \cdot ((2A - B) / 3))] - P_i r\alpha \tag{A.9}$$

$$A = [((1 + k)/2) \cdot (r + (a^2/r))] + [((1 - k)/2)\cdot(r - (a^4/r^3) + (4a^2/r))]\cos2\theta \quad (A.10)$$

$$B = [((1 + k)/2) \cdot (r - (a^2/r))] - [((1 - k)/2)\cdot(r - (a^4/r^3))]\cos2\theta \quad (A.11)$$

$$\alpha = (t / \eta_1) + (1 / E_1) + (1 / E_2)(1 - \exp(E_2 \cdot t / \eta_2)) \quad (A.12)$$

where P_i and P_o are an internal and external pressures, A and B are time-independent functions of position, K is bulk modulus, k is stress ratio, α is time-dependent function, θ is tangential coordinate, r is radius and a is inner boundary.
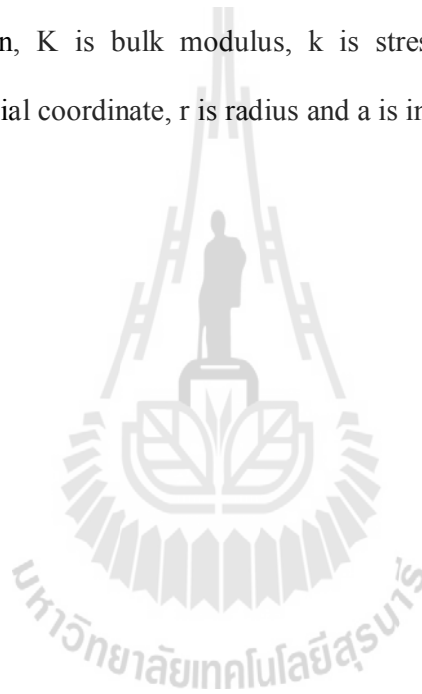
BIOGRAPHY

Mr. Sarayuth Archeeploha was born on January 21, 1984 in Bangkok province, Thailand. He received his Bachelor's degree in Engineering (Geotechnology) from Suranaree University of Technology in 2006 and Master's degree in 2009. During 2009-2010, he was a full time worker in position Geologist/Geotechnical engineer at Panya consultants Company Ltd., Bangkok. After that, he continued to study with degree of doctor of Philosophy in the Geological Engineering Program, Institute of Engineering, Suranaree University of Technology. During graduation, 2011-2015, he was a part time worker in position of research assistant at the Geomechanics Research Unit, Institute of Engineering, Suranaree University of Technology.